2012-12-20

Analysis and Modeling of Reserve and Regulation Prices in Competitive Electricity Markets

Wang, Peng

UNIVERSITY OF CALGARY

Analysis and Modeling of Reserve and Regulation Prices in Competitive Electricity Markets

by

Peng Wang

A THESIS

SUBMITTED TO THE FACULTY OF GRADUATE STUDIES

IN PARTIAL FULFILLMENT OF THE REQUIREMENTS FOR THE

DEGREE OF DOCTOR OF PHILOSOPHY

DEPARTMENT OF ELECTRICAL AND COMPUTER ENGINEERING

CALGARY, ALBERTA

December, 2012

Abstract

In a competitive electricity market, ancillary services, such as operating reserves and regulation service, are also traded, in addition to electric energy. The focus of the present thesis is on analyzing and modelling the prices of operating reserves and regulation services in competitive electricity markets.

Characteristics of the prices of reserves and regulation services in the Ontario, New York and ERCOT electricity markets are studied. More specifically, price variability, price jumps, long-range correlation, and non-linearity of the prices are analyzed using the available measures in the literature. The studied characteristics of operating reserve and regulation prices are also compared with those of energy prices. The findings show that the studied reserve and regulation prices feature extreme volatility, more frequent jumps and spikes, different peak price occurrence time, and lower predictability, compared to the energy prices.

To account for the distinguishing characteristics listed above, stochastic approaches for modelling the dynamics of operating reserve and regulation prices are investigated in the studied markets. Such descriptive stochastic models are necessary for risk management and derivative pricing of these commodities. Mean reverting jump-diffusion (MRJD) and Markov regime-switching (MRS) models with various specifications are analyzed. The performances of the two classes of models have been compared using various statistical measures.

Acknowledgments

I would like to first express my greatest gratitude to my supervisor Dr. Hamid Zareipour, who has provided me most valuable guidance and support in my research. I couldn't have completed this thesis without his help. The same appreciation is dedicated to my Co-supervisor Dr. Bill Rosehart for the great help in every aspects of my research and life during all my years in the University of Calgary. It was a great pleasure working with both of them.

Also I really appreciate my good friends who offered great help in my research and thesis writing, Tianyi Cai, Mamoud Mazadi, Ralph Liu, Daniel Huang, Han Yu. All of them have provided careful proofreading and valuable comments to my thesis and papers. I would like to specially thank my best friend and roommate Tianyi for his continuous encouragement and support in my busiest days when both my research and work reached the most important stages.

Last but not least, I would also like thank my beloved parents who have been most supportive to my study since I was a child. Their love is the source of my strength to overcome challenges.

This thesis is dedicated to my beloved family.

Table of Contents

List of Tables

List of Figures and Illustrations

Nomenclature

Indices:

t	Time
l	Time lag
k	Day
b	Base regime
s	Spike regime
d	Drop regime
$prior$	Prior probability
$post$	Posterior probability

Variables:

x_t	Price time series
r_{lt}	Logarithmic return
R_{lt}	Arithmetic return
W_t	Brownian motion component
J	Jump component
q_t	Poisson process
y_t	Integrated time series in DFA
X_t	Price time series variable
S_t	Stochastic component of the price
SE_{annual}	Annual seasonality
SE_{week}	Weekly seasonality
ma_t	Moving average

Ω_t	Observations up to time t
p_{ij}	Transition probability from regime i to j
$Prob$	Steady state probability

Parameters

ϕ	Phase angle in the sinusoidal function for annual seasonality
β	Mean-reversion rate parameter of the mean-reverting process
μ	Long-term mean parameter of the mean-reverting process
σ	Volatility parameter of the mean-reverting process
μ_j	Mean parameter of the Log-Normal distribution of the jump component
σ_j	Standard deviation parameter of Log-Normal distribution of the jump component
λ	Poisson distribution intensity parameter
μ_b	Mean parameter of the Log-Normal distribution of the base regime
σ_b	Standard deviation parameter of Log-Normal distribution of the base regime
μ_s	Mean parameter of the Log-Normal distribution of the spike regime
σ_j	Standard deviation parameter of Log-Normal distribution of the spike regime
μ_d	Mean parameter of the Log-Normal distribution of the drop regime
σ_d	Standard deviation parameter of Log-Normal distribution of the drop regime
p	Polynomial fit order in DFA
q	Norm parameter in DFA
τ	Time scale in DFA
θ	Parameter set of the MRS model

Abbreviations:

MRJD	Mean-reverting Jump-diffusion
MRS	Markov Regime-switching
TRS	Threshold Regime-switching
GARCH	Generalized Autoregressive Conditional Heteroskedasticity
ARMA	Autoregressive-moving-average
HVI	Historical Volatility Index
DVDA	Daily Velocity based on Daily Averages
DVOA	Daily Velocity based on Overall Averages
STD	Standard Deviation
DFA	Detrended Fluctuation Analysis
MLE	Maximum-likelihood Estimation
EM	Expectation-Maximization
ERCOT	Electric Reliability Council of Texas
HOEP	Hourly Ontario Energy Price
ONR10	Ontario 10-minute Spinning Reserve Price
ONR10n	Ontario 10-minute Non-spinning Reserve Price
ONR30	Ontario 30-minute Operating Reserve Price
LBMP6	New York Location Based Marginal Price of Zone 6
NYR10s	New York East Region 10-minute Spinning Reserve Price
NYR10n	New York East Region 10-minute Non-spinning Reserve Price
NYR30	New York East Region 30-minute Reserve Price
NYReg	New York Regulation Service Price
ERCOTRR	ERCOT Responsive Reserve Price
ERCOTRU	ERCOT Regulation Up Price

ERCOTRD	ERCOT Regulation Down Price
BS	Base-Spike
BSD	Base-Spike-Drop
BSE	Base-Spike Extreme
RVI	Relative Variation Index
PSD	Power Spectral Density
CDF	Cumulative Density Function

Functions:

$F_{p,q}$	Fluctuation function
$d(t)$	Deterministic component function
$N(\mu, \sigma)$	Normal distribution
$\exp$	Exponential function
Ln	Natural logarithm function
LogL	Log-likelihood function

Chapter 1

Introduction

1.1 Overview

Since the late 1990s, reform and restructuring of the electric power industry has been taking place in several countries around the globe. While electric energy is the dominant commodity in electricity markets, ancillary services are also traded in electricity markets. Ancillary services are required for the reliable and secure operation of electric power systems. Despite variations in the detailed definitions across markets, ancillary services include operating reserves, frequency regulation, reactive power for voltage support, and black start capability [1].

Market mechanisms and auctions for procuring ancillary services vary based on the nature of the service [2]. In general, services for which the requirements do not vary by operating conditions, or only a limited number of market players are eligible to provide them, are traded based on long-term contracts. Black start capability service is an example of this type of service, and is procured in a competitive manner in competitive electricity markets, such as the Electric Reliability Council of Texas (ERCOT) market and Ontario's market. On the other hand, those services, whose requirements change with operational conditions and many eligible suppliers may offer them, tend to be procured based on short-term auctions. In particular, operating reserves and frequency regulation service are usually procured competitively for each planning interval. For example, in Ontario's electricity market, three different classes of operating reserves are competitively procured by the system operator for each five-minute operation interval [3, 4].

Selling operating reserves and regulation services provides market players with business opportunities. Although the market volume for operating reserves and regulation is significantly smaller compared to that of electric energy, the profit gain for generation companies from these services can sometimes be comparable to that of electric energy [5]. This is particularly true for marginal and near marginal units for which the production costs and the revenue from selling energy are close.

The demand for operating reserves is traditionally driven by credible scenarios of forced generation and transmission line outages. Similarly, the demand for frequency regulation control depends mainly on unpredictable instantaneous variations of the electric load. The traditional suppliers of these services are flexible generation units, and in some limited cases, interruptible industrial loads (e.g., in the Ontario market [3]). However, with the growing integration of significant amounts of renewable energy generation resources into the grid, especially wind power, the grid faces another source of uncertainty, i.e., variability of supply. Thus, to accommodate this variable energy generation whose output is not completely predictable, the demand for operating reserves and regulation services is expected to grow [6, 7]. Moreover, the emerging smart grid paradigm is expected to further facilitate the provision of operating reserve and regulation services by non-traditional suppliers (e.g., distributed load entities) [8, 9]. Hence, with the increased activity in both the supply and demand sides of operating reserves and frequency regulation markets, modelling and analyzing the prices of these services in electricity markets is necessary.

With the increased importance of the ancillary services such as operating reserves and regulation services, an insight into the characteristics and variations of ancillary service prices is valuable for market players, as it provides a useful tool for risk management and derivative pricing. In this thesis, the characteristics of the reserve and regulation prices are extensively investigated in three North American electricity markets: the Ontario, New York, and Texas electricity markets. Stochastic models have been tested and a new model has been proposed for modelling these prices.

1.2 Background review

1.2.1 Significance of reserve and regulation service markets

Supplying energy, operating reserves and regulation services are the main sources of revenue for generation companies. Thus, several researches have focused on maximizing generation companies' total profit from selling energy, operating reserves and regulation services [10–14]. In addition, the advent of "smart grid" initiatives is expected to introduce new suppliers for reserve services (e.g., provision of reserves by electric vehicles) [8, 9, 15–17]. Also, large-scale integration of variable resources (e.g., wind) into the electric power systems may require more reserve and regulation services to ensure system security [6, 7, 18, 19].

1.2.1.1 Selling operating reserves and regulation services in competitive markets

Ancillary services are procured competitively, in conjunction with energy, in many electricity markets. Trading these services in the market provides the system operator another level of economic efficiency and technical flexibility. Several bidding and scheduling schemes have been proposed in the literature for generation companies to maximize profits in joint energy and ancillary services markets. For example, in [10], optimal allocation of the capacity of an electric energy supplier in the energy, reserve, and regulation markets is investigated. In [11], the self-scheduling problem of a power producer is formulated in order to maximize its total profit gained from supplying both the energy and reserve markets. A risk-constrained unit commitment model is proposed and solved in [12] for strategic bidding and self-scheduling of a generation company that participates in energy and reserves markets. In [13], a self-scheduling problem is developed for a generation company in order to maximize the profit of selling energy and reserve services while minimizing the total emissions. An optimal bidding framework in a pay-as-bid reserve auction is developed in [14]. As the future behavior of prices in electricity markets is not known in advance, the cited studies have employed various models to generate future price scenarios for energy and reserves and regulation services. Despite the variations in the types of models used, these studies have not distinguished between the characteristics of energy and reserve prices. However, as the demand for reserves and regulation services grows, more accurate models that properly describe the characteristics of reserve and regulation prices will be needed in order to optimize operation planning and investments.

1.2.1.2 The growing markets for operating reserves and regulation services

In recent years, the share of renewable energy resources, particularly wind, in electricity production has been growing at a significant rate [20]. Given the variable nature of wind power, several studies have focused on how reserve and regulation requirements of a system would change as a result of large-scale wind power integration. For example, in [6] it was demonstrated that, in an estimated future scenario, by integrating 10,000 MW of wind power into the Ontario system which has a peak system total demand of 26,000 MW, the required 10-minute operating reserve and regulation service were increased by about 51% and 11%, respectively. The increase of reserve requirements due to wind power integration for several regions, such as United Kingdom, Germany, and the Nordic region in Europe, and California and Minnesota in the United States, is summarized in [7]. According to [7], with a wind power penetration of 10% of the gross demand, the increases of reserve requirements may be as high as 15% of the installed wind capacity. Observe that depending on the characteristics of power systems, the extra reserve requirements as a result of wind integration may significantly vary. For instance, [7] reports that wind power integration has a minimal impact on reserve requirements in the New York market. However, in general, reserve requirements are likely to grow with large-scale wind power integration. Any increase in the demand for reserves and regulation services has an inevitable impact on the corresponding prices. Studies have also shown that wind power integration affects electricity market prices and system long-term reliability [21, 22].

On the supply-side of the reserves and regulation services, new opportunities are emerging within the context of smart electricity grids. For example, in [8], provision of operating reserves and regulation services by a fleet of Plug-in Hybrid Electric Vehicles (PHEVs) is investigated. In [15], supplying the peak power, spinning reserve and regulation service by electric vehicles is discussed, and the economics of such a practice are examined within the context of competitive electricity markets. Provision of spinning reserves using PHEVs to deal with the intermittency of wind generation is explored in [9]. Expansion of generation resources in the United States over the next 50 years is studied in [16], where PHEVs are considered as a provider of operating reserves required for balancing off wind variations. In [17], a PHEV aggregation model is proposed in order to provide regulation services and determine the optimal charging pattern of each vehicle. Obviously, the prices of reserves and regulation services play a critical role in the economic feasibility of using new technologies as providers of these services.

1.2.2 Characteristics of electric energy prices

The main characteristics of electric energy prices in various markets have been previously analyzed in the literature. For example, the variability of energy prices was quantified in terms of historical volatility and price velocity indices in [23–25]. As a popular measure of the variability of time series in finance, a historical volatility index was computed and studied in [23] for the electric energy prices in the Nordic market. Significantly higher volatilities were found for electricity market prices compared to those of other markets, such as stock markets. Price velocity indices were proposed in [24] as an alternative measure of the variability of energy prices. While price volatility focuses on variability of the variance of price fluctuations, price velocity quantifies the changes of the prices themselves. In [25], both the historical volatility and price velocity indices were employed and extended to different time scales to investigate the variability of the energy prices in the Ontario electricity market. It was reported in [25] that the variability of Ontario electricity prices was the highest compared to its neighbouring markets. In addition, jumps and spikes [26–28], mean-reversion and long-range correlation [28, 29], and non-linearity of energy prices [29] have been studied in the literature.

While the characteristics of energy prices have been widely addressed in several studies, the literature on analyzing reserve prices is limited. In [30], statistical characteristics of daily energy and reserve prices in the German electricity market were studied. It was found in this paper the reserve prices in the German market don't follow normal distribution and have regime-switching property.

1.2.3 Modelling prices in competitive electricity market

Modelling energy prices in competitive electricity markets have been widely investigated in the past decade, with various models proposed and compared [26, 28, 31–43]. Most of the existing studies decompose electricity prices into two components, a deterministic component and a stochastic component. The deterministic component usually represents the long-term trend and seasonality, while the stochastic component represents the stochastic fluctuations [31]. The stochastic component requires an appropriate model to capture the main characteristics of the electricity price stochastic dynamics, which include mean-reversion, spikes, and non-constant volatility.

Starting from the basic mean-reverting process, which is also called the Ornstein-Uhlenbeck process [32], various specifications have been proposed to capture the above characteristics of energy prices. The simple mean-reverting process is usually not sufficient to represent dynamics in the energy prices, because mean-reversion rate and volatility are assumed to be constant in this model. This assumption is not valid when jumps and spikes occur, which widely exist in electric energy price. Depending on how mean-reversion rate and volatility variations are modelled, there are other models that have been most popular for electric energy prices.

The mean-reverting jump-diffusion (MRJD) model is an extension of the Ornstein-Uhlenbeck model by adding a separate jump component [26, 33, 35]. The jump component is represented by a Poisson process which generate the the occurrence of jumps or spikes, and a probability distribution which models the size of the jumps. Log-Normal distribution is more appropriate than Gaussian distribution for jump size, as it has fatter right tail which is consistent with the distribution of jumps [44].

The MRJD models are capable of capturing jumps and spikes, but one deficiency is that jumps can result in a much biased mean-reversion rate. When price return from spikes to the normal price state they need a very large mean-reverting rate, which will cause a biased estimate of this parameter. In [33], a potential function was used to enable varying mean-reversion rate. Another solution is to make the jump process independent of the normal price process [26, 36].

One deficiency of MRJD models with independent jumps is lack of capability to generate consecutive jumps or spikes, a phenomenon which has been frequently observed in electricity market prices. As an alternative, regime-switching models, which are able to deal with this problem, have been proposed and have achieved successful applications. Regime-switching models represent the prices by multiple regimes, and prices can transit between regimes. Depending on the transition law, regime-switching models can be further classified into Markov regime-switching models (MRS) and Threshold regime-switching models (TRS). The MRS models have been found to better fit the objective of price modelling, and are the most popular models utilized for energy price modelling in recent years. A three-regime model has been proposed in [34] in which, the jump behaviors are modelled by one jump-up regime and one jump-down regime, and the normal state of the price is modelled by another regime. The research in [37] has utilized this three-regime model for the energy price in the Australian market. This three-regime model assumes the spikes are not consecutive, i.e., a spike will jump back to the normal price in the next time interval after it occurs. However, this assumption is not always correct, as shown in [45]. A three-regime model that allows consecutive spikes is used in [40] and has shown better accuracy than the restricted three-regime model in [34]. Several two-regime MRS models are used in [26,38,39] that represent the price by one normal regime and one independent spike regime. The normal regime of the above two-regime and three-regime MRS models are represented by a mean-revering process. The spike regime is modelled by Gaussian [34, 37] or Log-Normal [26, 39] distributions. The Pareto distribution is proposed to model the spike regime in [46], but it does not outperform the models with Log-Normal or Gaussian distributions. The work in [47] has proposed a two-regime model that employs a shifted Log-Normal distribution for the spike regime to avoid that the spike regime captures drops in price process. This model is later extended to a three-regime base-spike-drop model by adding a regime to capture the drops [41]. Both two-regime and three-regime models have been discussed in [38, 40, 41] and compared, concluding that performance highly depends on the price data under study.

On the other hand, the TRS model has been proposed in [48] which identifies regime transitions by pre-specified thresholds. In [38], MRS and TRS models have both been applied to energy prices and compared. The numerical results showed that the MRS outperforms the TRS model in modelling energy price. However, the TRS model has shown better performance than the MRS model in forecasting energy prices [49].

Other models have also been proposed and applied to electric energy prices. For example, another popular class of models that has been applied to electric energy prices is the generalized autoregressive conditional heteroskedasticity (GARCH) model. GARCH models allow time-varying variance and were studied and compared with other models in [38, 42]. As discussed in [38], GARCH models assume that variance changes in the prices are moderate. However, this may not be the case in electricity reserve prices where frequent extreme jumps are observed. The research in [43] proposed a spectral model built in frequency domain. While most existing studies have focused on daily prices, there are some studies on hourly prices. In [35], several models, including MRJD and GARCH models, are applied to hourly energy prices from California. Most of the existing work built models for log-prices, but [39] has shown that modelling actual prices can sometimes achieve a better fit.

Exogenous variables have been introduced to increase the accuracy of modelling energy prices. In [50], regime-switching models are developed and exogenous variables, such as demand and generation capacity margin, are used to represent the prices under each regime. A three-regime model with one base regime and two spike regimes is used for the most volatile period of price. The work in [51] employed demand and weather variables in the regime-switching model for energy prices in Queensland. However, the demand of reserve and regulation services is dictated by the system operation conditions, and the system operation data are not always available to the public. Therefore, this thesis focuses on the stochastic models that only rely on the price itself, and thus the exogenous variables are not considered. However, the models applied in this thesis are flexible to be extended to include exogenous variables.

In summary, the MJRD model with independent jumps and the MRS model are the two that tend to capture the frequent sudden jumps or spikes in price series. Therefore, these models are selected as candidates for reserve and regulation prices in the studied markets.

In [30], statistical characteristics of daily energy and reserve prices in the German electricity market were studied and non-normality and regime-switching properties were reported for reserve prices. An Autoregressive-moving-average (ARMA) model was used and extended in the way that the error term was modelled. Various models were tested for the error term, including the regime-switching scheme.

1.3 Motivation and Objectives

1.3.1 Characteristics of prices in competitive electricity market

Characteristics of energy prices in competitive electricity markets have been widely explored [23–25, 27–29], and several price forecasting models have been proposed [52, 53]. However, the existing literature on analysis of reserve prices is limited [30]. One of the objectives of this thesis is to analyze the characteristics of hourly prices of operating reserves and regulation services. More specifically, operating reserve and regulation prices are analyzed for their variability, price jumps and extreme prices, non-linearity and long-range correlations. Furthermore, characteristics of the operating reserve and regulation prices are compared with those of the hourly energy prices in the respective markets, where possible. Electricity markets of Ontario, New York and Texas are used as test markets. The analysis is aimed at:

1. Revealing the distributional characteristics and patterns of the reserve and regulation prices in three North American electricity markets.

2. Providing a quantitative insight and evaluation of statistical characteristics of the studied prices, including variability, jumps/spikes, and long-range correlation for the studied prices.

3. Presenting a comparative analysis of the studied prices among the subject markets.

The findings of this part of the thesis (Chapter 3) provide insights into the characteristics of the reserve and regulation prices, which are useful for operation and planning activities in a competitive electricity market.

1.3.2 Stochastic models for reserve and regulation prices

Although the modelling of energy prices has been widely studied, the existing literature that focused on modelling reserve prices is limited [30, 54]. The other objective of this thesis is to investigate the effectiveness of MRJD and MRS approaches in modelling daily average and hourly prices of operating reserves and regulation service in competitive electricity markets. These two classes of approaches have shown promising results of modelling electricity energy prices. Specifically, this part of the thesis (Chapter 4 and Chapter 5) aims at:

1. Exploring the applicability of some of the most established stochastic models in capturing the characteristics of reserve and regulation prices in typical North American electricity markets.

2. Providing a comparative analysis on the effectiveness of stochastic models for the energy prices and for reserve and regulation prices.

Such price models are important for pricing derivatives and risk management in practical reserve and regulation markets. Note that such models are descriptive and may not be suitable for short-term hour-to-hour prediction.

The characteristics and models studied in this thesis can provide useful information to both the system operator and market participants to better understand, and estimate future behaviour of, the reserve and regulation prices in the electricity market and make strategy to hedge the financial risks.

1.4 Outlines of the thesis

- **Chapter 2** - This chapter provides a mathematic background review of the main methods, algorithms, and models applied in this thesis. More specifically, the methods and indices used for statistical analysis of the prices are introduced. The processes of modelling the deterministic and stochastic components of the price time series are also demonstrated. Two classes of models for the stochastic component, being the mean-revering jump-diffusion (MRJD) and Markov regime-switching (MRS) models, are introduced in this chapter.

- **Chapter 3** - The statistical characteristics of the reserve and regulation prices are studied by descriptive statistics, patterns, variability, jumps and spikes, and long-range correlation. The differences between energy prices and reserve and regulation prices, with respect to these measures, are analyzed, and origins of these differences are discussed.
- **Chapter 4** - Dynamics of the daily averages of the studied prices are modelled in this chapter. Three stochastic models, i.e., one MRJD model and two MRS models, have been selected based on the characteristics of the studied reserve and regulation prices. The three candidates of models are applied to the studied prices, and their performances are evaluated and compared.
- **Chapter 5** - This chapter is dedicated to modelling price dynamics for hourly reserve and regulation prices. Several MRS models are selected and tested for the prices. In addition to the tradition that the price models are built for log prices, modelling the original prices before logarithmic transformation has also been explored. A new model has been proposed to capture the distinguishing features in the hourly reserve price.
- **Chapter 6** - The main contributions of this thesis are summarized in this chapter.

Chapter 2

Background Review

2.1 Introduction

In this chapter, measures, algorithms, methods, and models applied in this thesis are reviewed. The measures to evaluate the statistical characteristics are first introduced in Section 2.2. Variability indices, the jump identification algorithm, and the long-range correlation analysis method are introduced in this section and are applied to the studied prices in Chapter 3. The price modelling procedures are introduced in Section 2.3. The decomposition of deterministic and stochastic components from the price time series is introduced in detail in this section. The stochastic models that are applied to the reserve and regulation prices in this thesis are presented in Section 2.4. Calibration techniques for these models are also presented in this section, and are used in Chapter 4 and Chapter 5 to estimate the parameters of the stochastic models.

2.2 Measures for statistical characteristics

In this thesis, statistical characteristics including variability, jumps and spikes, and long-range correlation are investigated to distinguish the reserve and regulation prices from energy prices. The measures, indices and analysis methods are introduced in this section.

2.2.1 Variability

Historical volatility index and price velocity are two major classes of indices to quantify variability. The calculation of these indices are introduced below.

2.2.1.1 Historical volatility index

To study the variability of a given time series, historical volatility is a popular measure in the finance literature [55, 56], and hence, it has been applied to electricity market prices [23, 25]. Historical volatility index is calculated as the standard deviation of the price returns with a given lag [55, 56]. The price returns, being relative price changes, can be taken in logarithmic or arithmetic form of a time series. Let x_t be the price at time t. The logarithmic return is computed as:

$$r_{lt} = \ln x_t - \ln x_{t-l} \tag{2.1}$$

And the arithmetic return is

$$R_{lt} = [x_t - x_{t-l}]/x_{t-l} \tag{2.2}$$

l in the above equations (2.1) and (2.2) is the time lag (e.g., $l = 24$ represents daily price returns for hourly prices). The total length of the price time series is divided into N windows, each with a length T. Then the standard deviation of x_t in window n is calculated as:

$$\sigma_{l,T}(n) = \sqrt{\frac{\sum_{t=(n-1)\times T+1}^{n\times T}(R_l(t) - \overline{R}_{l,T}(n))^2}{T-1}} \tag{2.3}$$

where $\overline{R}_{l,T}(n))$ is the average of the the price return in the current window n. The historical volatility index (HVI) is calculated as the average of the standard deviations in (2.3) over all windows, i.e.,

$$HVI = \frac{1}{N}\sum_{n=1}^{N}\sigma_{l,T}(n) \tag{2.4}$$

2.2.1.2 Price velocity index

Another class of indices used in this thesis is the price velocity, which was proposed in [24] to investigate the variability in energy prices from 14 electricity markets and extended in [25] to study the variability of energy price in Ontario's and its neighboring markets. Price velocity measures the ratio of average price changes with respect to the overall average or daily average of the price.

To compute price velocity, first, the changes in prices are calculated as $\delta_{lt} = |x_t - x_{t-l}|$. Two price velocity indices are usually used, namely, daily velocity based on daily averages (DVDA) and daily velocity based on overall averages (DVOA) [24]. In this thesis, only the DVDA index is presented because the results of the two indices were found to be consistent for the studied prices. The DVDA index is defined as [24]:

$$\text{DVDA}_l^{(k)} = \frac{\overline{\delta}_{lt}^{(k)}}{\overline{x}^{(k)}} \tag{2.5}$$

where, $\overline{\delta}_{lt}^{(k)}$ is the daily average of δ_{lt} for day k, and l is the time lag, i.e., 1, 24 and 168 hours to study intra-day, inter-day, and inter-week price velocities as in [25]. The values of $\text{DVDA}_l^{(k)}$ are averaged over all days in the studied period, and are denoted by $\overline{\text{DVDA}}_l$.

2.2.2 Price jump identification

The occurrences of jumps are identified by a jump filtering algorithm following [26, 36]. For a price time series x_t of length n, The jumps are first identified as the price changes that exceed a threshold, defined as:

$$\Delta x_t = x_t - x_{t-1} > \overline{\Delta x_t} + \alpha \times STD(\Delta x_t) \tag{2.6}$$

where, $\Delta x(t)$ is the price change at time t with $t = 2, 3, ..., n$; $\overline{\Delta x(t)}$ is the average of all price changes, and it is usually close to zero for electricity price; and, $STD(\Delta x_t)$ is the standard deviation of all price changes Δx_t. The typical values of α include 2.5 and 3 [26, 36], and 3 is picked here. Any Δx_t that is greater than the threshold $\overline{\Delta x_t} + \alpha \times STD(\Delta x_t)$ is identified as a price jump. The identified jumps are replaced by the threshold to remove the jumps from the price series. The filtering process based on (2.6) is repeated until no more jumps are detected as in [33, 36]. The purpose of repeating the filtering is to avoid situations where a few super extreme price changes raise the threshold to a high level. Only the upward jumps are identified here which usually lead to the extremely high prices.

The number of identified price jumps are then divided by the sample size of the corresponding price process to obtain the frequency of jump occurrence, i.e., f_{jump}.

2.2.3 Detrended fluctuation analysis

Detrended fluctuation analysis (DFA) has been utilized in finding long-range correlation and identifying mean reversion in electricity prices [28, 29]. Compared to other methods such as the R/S method [28], DFA performs better in exploring intrinsic dynamics in non-stationary time series [29, 57]. DFA calculates the generalized Hurst scaling exponent $H_{p,q}$ to represent the fractal characteristic, where p is the order of polynomial fit, and q is the order of norm taken during the calculation of $H_{p,q}$. The procedures of DFA are briefly introduced below. More details can be found in [29, 57, 58].

1. The time series x of length N is first integrated as $y_t = \sum_{i=1}^{t} |x_i - \bar{x}|$, $t = 1, ..., N$, where $\bar{x}$ is the average of the time series x.

2. The integrated time series y is divided into windows with a window length m. For the jth window, the sub-series is written as $y_j(m, t)$, and the time scale of each window is $\tau = m\Delta t$ where Δt is the sampling period.

3. The local trend in each window is obtained by calculating the polynomial fit of order p for each sub-series $y_j(m, t)$, denoted as $y_j^{poly}(m, t)$. The polynomial fit is subtracted from $y_j(m, t)$ in each window to get the detrended time series in each window as $d_j(m, t) = y_j(m, t) - y_j^{poly}(m, t)$ for window j. $d_j(m, t)$ represents the fluctuation component of $y_j(m, t)$ after being detrended in window j with window length m.

4. When the detrending step is done for every window, the fluctuation function

is computed as the q-norm of the detrended fluctuation sequence $d(m,t)$:

$$F_{p,q}(m) = (\frac{1}{M}\sum_{j=1} M|d_j(m,t)|^q)^{1/q} \tag{2.7}$$

Since $\tau = m\Delta t$, $F_{p,q}$ is a function of τ as well, and thus can be written as $F_{p,q}(\tau)$.

5. If the power-law scaling behavior can be observed as $F_{p,q}(m) \sim \tau^{H_{p,q}}$, then the $H_{p,q}$ is called the generalized Hurst-scaling exponent. Thus, the $H_{p,q}$ is computed as the slope of the logarithmic $F_{p,q}(m)$ versus logarithmic m.

A $H_{p,q}$ value of less than 0.5 indicates there is a negative auto-correlation in x, while a $H_{p,q}$ value of between 0.5 and 1.5 indicates positive auto-correlation, and $H_{p,q} = 0.5$ corresponds to a random walk [57].

2.3 Modelling prices in electricity market

The general form of the proposed models for electric energy prices in the literature (e.g., [26, 38, 40]) is:

$$X_t = d(t) + S_t \tag{2.8}$$

X_t is the price process of interest, being the observations of the price from a historical period. $d(t)$ is the predictable deterministic component, which is a function of time t. The deterministic component usually contains a seasonality component and a linear trend. s_t is the stochastic component which represents the non-predictive price dynamics. A large number of research works have focused on building models for the stochastic component.

2.3.1 Modelling the deterministic component

As stated above, the price process is first decomposed into a deterministic component and a stochastic component. The identification of deterministic component is introduced in this section and the modelling of stochastic component will be introduced in the next section.

The deterministic component usually contains a linear trend that represents long-term price evolution, and a seasonality component that represents the periodical fluctuations in the prices.

For electric energy prices, the model of the deterministic component can be written as follows:

$$d(t) = SE(t) + kt + b \tag{2.9}$$

On the right side of (2.9), the first component is the seasonality, and the rest is the linear trend.

Seasonality is a property that the price fluctuates following periodic cycles. Seasonality has been widely observed in electric energy prices, and usually consists of daily, weekly, and annual cycles. One popular method to model the annual seasonality component is to represent it by sinusoidal function. For daily prices, the sinusoidal function can be written as:

$$SE_{annual} = Msin(\frac{2\pi}{365}t + \phi) \tag{2.10}$$

M is the amplitude of the annual component, and the number 365 defines the period is one year. When modelling hourly prices, the number 365 will change to 8760, which is the number of hours in a calendar year.

The daily and weekly seasonality identifications in this thesis employ a moving average technique following [26, 28]. Take the weekly seasonality as an example, for a daily time series x_t, the moving average is calculated first:

$$ma_t = \frac{1}{7}\sum_{i=-3}^{3} x_{t-i} \tag{2.11}$$

Then the deviation between x_t and ma_t is calculated, and the average of the deviations is calculated for each entry of the seasonality cycle. For a weekly seasonality, the average is calculated for each of the seven days of a week. Denote the deviation average of day j is

da_j, then the weekly seasonality component of day j is calculated as:

$$SE_{week}^{j} = da_j - \frac{1}{7}\sum_{i=1}^{7} da_j \tag{2.12}$$

After this calculation is repeated for each of the seven days, the weekly seasonality vector is obtained.

2.3.2 Modelling the stochastic component

The stochastic component of a price time series is the essential part for applications in risk management and derivative pricing. A large number of stochastic models have been proposed and examined for energy prices in electricity markets. Several of them have been reported to perform better than others with respect to modelling the main characteristics of energy prices, such as mean-reversion and spikes, and are thus selected as candidates for modelling reserve and regulation prices. These stochastic models are introduced in detail in the next section.

2.4 Stochastic component modelling

As discussed above, the price time series is first decomposed to deterministic and stochastic components. The stochastic models are then applied to the stochastic component to describe the price dynamics. Logarithmic transformation is usually taken on the stochastic component first before the stochastic models are applied. However, there are a few papers that have directly modelled the original stochastic component [39, 41]. In the following context, S_t denotes the stochastic component to be modelled, while it can be either original price or log price.

The basic Ornstein-Uhlenbeck mean-reverting process which is used in [32] to model energy price in electricity markets and can be presented as follows:

$$dS_t = \beta(\mu - S_{t-1})dt + \sigma dW_t \tag{2.13}$$

where, the S_t is the stochastic component of the log price. In this model, the first component on the right hand side drives the price to go back to its long-term average level μ when the price departs from it. The mean-reversion rate β determines how fast the price will go back to μ. W_t in the second component is a standard Brownian motion, which accounts for random moves in the price process. σ is volatility, which determines the size of the random walk.

The basic Ornstein-Uhlenbeck process is able to represent the mean-reversion property that has been widely observed in electricity prices. However, the existence of pronounced spikes or jumps, which is another characteristic of electric energy, reserve, and regulation prices, is not well covered. Since the parameters in (2.13) are constant over time, price spikes would bring distortions to the mean, volatility and mean-reversion rate [59]. These biased parameters may not appropriately represent the characteristics of non-spike prices. Thus, in the recent literature [26, 38, 41], this mean-reverting process is used to model the normal state of prices, i.e., the state that prices evolve relatively smoothly without jumps.

Since reserve and regulation prices have more frequent spikes and more extreme prices compared to energy prices [54], an appropriate solution to incorporate jumps in the model is a critical requirement. The MRJD and MRS models are good candidates in this sense, which have been previously applied to energy prices. The MRJD model adds a separate jump component for jumps and spikes, while the MRS model recognizes independent states/regimes in the price process and utilizes different processes to represent the regimes. The MRJD and MRS models [28] are introduced in the following subsections, and are applied to the studied reserve and regulation prices in this thesis.

2.4.1 MRJD model

The MRJD model models the jumps in prices as a separate component added to the normal price process, as:

$$dS_t = \beta(\mu - S_{t-1})dt + \sigma dW_t + J_t dq_t \tag{2.14}$$

where the last component in (2.14) is the jump component. The rest portion of the right side in (2.14) is a mean-reverting process defined in (2.13), which is used to represent the normal price process. q_t in the jump component is a Poisson process with intensity λ which accounts for the occurrence of jumps. J_t determines the size of the jump, and is usually modelled by probability distribution that has a right tail, such as a Log-Normal distribution [26, 44], i.e., $\ln J \sim N(\mu_j, \sigma_j)$. The mean of the Log-Normal distribution is calculated as $\exp(\mu_j + \sigma_j^2/2)$.

MRJD models treat the jumps/spikes as a separate component; this allows for sudden jumps appearing in the process. Furthermore, the impact of jumps on the normal process's parameters is reduced. This is because the jump component has its own parameters to model the large size and dispersion of the jumps. However, in daily electricity prices, the price spikes usually only last for very short periods, and will jump back to normal level after that. In this case, when the price jumps from a spike size back to normal, a strong driving force is needed to make such a big drop in price. The driving force has to be provided by the mean-reversion parameter β. Thus, the jump back from a spike tends to need an excessive mean-reversion rate, and hence, will drive the parameters β higher than required by the normal price process. As a result, the estimated mean-reversion rate tends to be not suitable to represent the price dynamics in non-spiky periods, i.e. the mean-reversion rate will be shifted up by jumps. One solution to the shifted mean-reversion rate is to have a jump component that is independent of the mean-reverting process, i.e., the normal price process. This model is introduced next.

2.4.1.1 MRJD model with independent jump component

As discussed above, a MRJD model with an independent jump component is immune to the problem that the mean-reversion rate is shifted by the jumps. Such models have been proposed and applied to electricity energy prices in [26, 33]. Having an independent jump component is equivalent to forcing the price to jump back to the normal price level immediately after it occurs, and thus relieves the need of a high mean-reversion rate to drive the force back to normal.

2.4.1.2 Calibration of MRJD model

To calibrate the MRJD model with independent jump component, the jumps and normal price process are calibrated separately. The first step is to separate the jumps from the normal prices by the filtering algorithm presented in Section 2.2.2.

The filtered jumps in the first step is then fit by a Log-Normal distribution to calculate the μ and σ of the jump size random variable J. The frequency of the Poisson process, denoted as λ, is calculated as the frequency that jumps occurred in the price process. If m jumps occurred in N observations, the frequency is:

$$\lambda = \frac{m}{N} \tag{2.15}$$

After removing the jumps, the mean-reverting portion of the model in (2.14), i.e., the portion that equals to the mean-reverting model (2.13), is then calibrated to fit the normal price process by maximum-likelihood estimation (MLE).

The log-likelihood function of the MRJD model will be a combination of the log-likelihood functions of the normal process and the jump component. The log-likelihood function of the normal process is the same as in (2.13), while the log-likelihood function of the jump component is calculated based on the probability density function of the distribution used for the jump size.

The derivation of the likelihood function of the mean-reverting process is introduced next. The mean-reverting portion of the stochastic differential equation in (2.14), i.e., the equation (2.13), can be discretized with step size 1, and it becomes:

$$S_t - S_{t-1} = \beta(\mu - S_{t-1}) + \sigma dW_t \tag{2.16}$$

Then the first component on the right hand side of the equation is moved to the left side, and for simplicity in presentation, consider the following notation:

$$e_t = S_t - S_{t-1} - \beta(\mu - S_{t-1}) \tag{2.17}$$

then (2.16) becomes:

$$e_t = \sigma dW_t \tag{2.18}$$

Since W_t follows a standard normal distribution, e_t follows a normal distribution $N(0, \sigma)$. The likelihood function at time t is calculated as the probability density function of the normal distribution, as follows:

$$L_{mr,t}(\theta) = f(e_t; \sigma) = \frac{1}{\sqrt{2\pi}\sigma} exp[-(\frac{e_t^2}{2\sigma^2})] \tag{2.19}$$

where, θ is the set of parameters. For the mean-reverting model $\theta = \{\beta, \mu, \sigma\}$. Thus, the likelihood function of the entire data set S_t, t=1,2,...,T, is:

$$L_{mr} = \prod_{t=1}^{T} L_{mr,t} \tag{2.20}$$

The log-likelihood function is as follows:

$$LogL_{mr}(\theta) = \sum_{t=1}^{T} \ln f(e_t; \sigma) \tag{2.21}$$

$$= \sum_{t=1}^{T} -\frac{1}{2}e_t^2 - \ln\sigma - \frac{1}{2}\ln 2\pi \tag{2.22}$$

Since the jump component is independent of the normal process, the log-likelihood function of the MRJD model is the summation of the log-likelihood functions of the normal process and the jump component, as follows:

$$LogL_{MRJD} = LogL_{mr} + LogL_j \tag{2.23}$$

where, $LogL_j$ is the log-likelihood depending on the distribution used to model the jump size. $LogL_j$ is calculated as the summation of the probability density functions of all jumps identified by the filtering algorithm.

2.4.2 MRS model

The Markov regime-switching (MRS) model recognizes that there are multiple regimes or states in the price process. This class of models have been used for modelling electric energy prices since a multi-regime behavior has been observed in those prices. For example, when an outage of generator or major transmission line occurs, the price tends to jump up to a much higher level. These models are also applied to the reserve and regulation prices in this thesis because multi-regime dynamics have been found in these prices as well.

The MRS uses a latent variable R to represent the regime that the price currently resides in. For a MRS model that has n regimes, $R = 1, 2, ..., n$. Since the increased number of regimes would require a higher computation burden, the two-regime and three-regime models are most popular in electricity price modelling.

Both the two-regime and three-regime specifications of MRS models tend to categorize the prices into a base regime and one or two excited regimes. The base regime captures the normal prices with moderate fluctuations, while the excited regimes model the prices that are obviously away from normal level. The base regime usually captures most observations in the price process. The two-regime models represent prices by a base regime and a jump/spike regime, while the three-regime models add a drop regime.

Transition between regimes are modelled by a Markov chain. The price may transfer from one regime to another at any time with a transition probability. The transition probability is a conditional probability depending on the regime in which the process currently resides. A transition probability matrix contains transition probabilities; an example of transition probability matrix for a 2-state Markov chain is as follows:

$$P = \begin{bmatrix} p_{11} & p_{12} \\ p_{21} & p_{22} \end{bmatrix} \tag{2.24}$$

Each row corresponds to the current regime and each column corresponds to the regime after one time interval. For daily prices, the column corresponds to the regime of the price of next day. Assuming the two regimes are labeled by 0 and 1, if the current regime is 0, the probability of staying at this regime is p_{11} and the probability of transferring to regime 1 is p_{12}. Similarly, if the current regime is 1, the probability of staying at the current regime is p_{22} and transferring to regime 0 is p_{21}. Since the probabilities in a row i represent all possible transition from regime i, the summation of these probabilities equal to one, i.e., $\sum_j p_{ij} = 1$.

The MRS model applied in this thesis deploys a mean-reverting process as in (2.13) for base regime. For the spike regime the Log-Normal distribution and Gaussian distribution are tested. These specifications have been applied in the literature [28] and reported to be suitable for energy prices. An example of two-regime MRS model is presented in (2.25) with a base regime and a spike regime. The base regime is modelled by a mean-reverting process, and the spike regime is represented by a Log-Normal distribution.

$$\text{Base Regime: } dS_t = \beta_b(\mu_b - S_{t-1})dt + \sigma_b dW_t \tag{2.25a}$$

$$\text{Spike Regime: } \ln(S_t) \sim N(\mu_s, \sigma_s) \tag{2.25b}$$

The MRS class of models have been reported to have better fit than MRJD models for energy prices in most comparisons [26,38,40]. However, for some energy prices, the MRJD models can have comparable performance as the MRS models, such as for the prices in the Nordic Pool and Austria markets in [40]. Therefore, in this thesis, both these two classes of models are tested, each with various specifications. The performance of the various models are compared to find the more appropriate model for the reserve and regulation prices.

2.4.2.1 MRS two-regime model with shifted spike

The MRS two-regime model in (2.25) has a deficiency that its spike regime may capture not only positive spikes but also drops in prices. This deficiency can distort the parameters of the spike regime and the transition probabilities, and thus result in misleading model parameters. This model has the deficiency because the optimization of log-likelihood function tend to assign any prices that seem not to belong to the base regime to the spike regime. Since sometimes the drops are also significantly far way from normal prices, they may be assigned to the spike regime.

A MRS model with shifted spikes was proposed in [47] to solve this problem. The shifted spike regime applies a threshold of spike identification, denoted as TS, to avoid the spike regime capturing any price under the threshold. The MRS two-regime base-spike model with shifted spike regime is presented as follows:

$$\text{Base Regime: } dS_t = \beta_b(\mu_b - S_{t-1})dt + \sigma_b dW_t \tag{2.26a}$$

$$\text{Spike Regime: } \ln(S_t - TS) \sim N(\mu_s, \sigma_s) \tag{2.26b}$$

It should noted that although a threshold is applied, the spikes are still identified through optimizing log-likelihood function. The prices above the threshold TS are not necessarily captured by the spike regime. TS is set as the median of the price process to be modelled. Therefore, any price under the median of S_t won't be identified as spikes. The mean of the spike regime implied by the model is the summation of TS and the mean of the Log-Normal distribution, i.e., $TS + \exp(\mu_s + \sigma_s^2/2)$.

2.4.2.2 MRS three-regime model with shifted spike and shifted drop

The MRS two-regime base-spike model with shifted spikes have solved the problem that drops are identified as spikes. However, the drops are assigned to the base regime, which will distort the base regime parameters. In [41], a three regime model is proposed to separately model the prices significantly lower than the normal prices by a drop regime. Similar to the shifted Log-Normal distribution used for the spike regime, the drop regime also employs a threshold TD to avoid mis-capturing of drops. Only prices that are below TD can be identified as a drop. This MRS three-regime base-spike-drop model is presented as follows:

$$\text{Base Regime: } dS_t = \beta_b(\mu_b - S_{t-1})dt + \sigma_b dW_t \tag{2.27a}$$

$$\text{Spike Regime: } \ln(S_t - TS) \sim N(\mu_s, \sigma_s) \tag{2.27b}$$

$$\text{Spike Regime: } \ln(TD - S_t) \sim N(\mu_s, \sigma_s) \tag{2.27c}$$

Similar to the shifted spike regime, the threshold of drops TD is set as median of the price to be modelled. As presented in Section 2.4.2.1, the mean of the spike regime implied by the model is $TS + \exp(\mu_s + \sigma_s^2/2)$, and similarly the mean of the drop regime is $TD - \exp(\mu_d + \sigma_d^2/2)$.

2.4.2.3 Calibration of MRS model with expectation-maximization (EM) method

The MRS models are usually calibrated with the expectation-maximization (EM) method, which has been presented in detail in [38, 60–62]. There two steps in this method, the expectation step and maximization step. In the first step, the expectation of the likelihood function is calculated as weighted average of all regimes. In the latter step, the MLE method is implemented to estimate the new set of parameters that maximizes the expectation calculated in the first step. The detailed procedures of the two steps of the EM method, i.e., the expectation step and the maximization step, are introduced next for a time series time series x_t with length T, i.e., $t = 1, 2, ..., T$.

1. Expectation step

   In the expectation step, the likelihood function is calculated as expected value of likelihood functions of all regimes. Probabilities of residing in each regime are used to calculate the expected value. This calculation uses prior and posterior probabilities and the log-likelihood function of each regime.

The prior probability at time point t is the probability before accounting for the observation at the current time point t. And the posterior probability is the probability that has taken account of the observation at time t.

Take a two-regime model as an example, regime parameter $r = 1, 2$. Denote the prior probabilities at time t as ξ_{jt}^{prior} and the posterior probabilities at time t as ξ_{jt}^{post}, where $j = 1, 2$. The prior probability can be calculated from the posterior probability at the last time point, $t-1$, by:

$$\xi_{jt}^{prior} = \sum_{i=1}^{2} \xi_{i,t-1}^{post} p_{ij} \tag{2.28}$$

where $i = 1, 2$ is the regime at the previous time point $t-1$.

The posterior probability of a price being at regime j at time t, given the set of observations up to time t, denoted as Ω_t, and the set of parameters, denoted as θ, is:

$$\xi_{jt}^{post} = Pr(r_t = j)|\Omega_t; \theta) \tag{2.29}$$

Note that $\sum_j s_{jt} = 1$. In the case of 2 regimes, the summation of ξ_{1t} and ξ_{2t} is one.

The posterior probability ξ is calculated from the prior probability and the probability density function $f(x_t|s_t = j, \Omega_t; \theta)$ defined by the the specification of the model, as follows:

$$\xi_{jt}^{post} = \frac{\xi_{jt}^{prior} f(y_t|s_t = j, \Omega_t; \theta)}{\xi_{1t}^{prior} f(x_t|r_t = 1, \Omega_t; \theta) + \xi_{2t}^{prior} f(x_t|r_t = 2, \Omega_t; \theta)} \tag{2.30}$$

The posterior probabilities ξ_{jt}^{post} at time t are calculated based on the observations up to the time t, Ω_t. After the ξ_{jt}^{post} is calculated for all time points up to length T, the posterior probability can be calculated based on the entire set of observations, i.e, Ω_T, through a backward iteration for $t = T-1, T-2, ...1$:

$$\xi_{jt}^{T} = \sum_{i=1}^{2} \frac{\xi_{jt}^{post} \xi_{i,t+1}^{T} p_{ji}}{\xi_{i,t+1}^{prior}} \tag{2.31}$$

The ξ_{jt}^{T} is then used as the probability that x_t is at regime j at time t to evaluate the expectation of the likelihood function of the MRS model.

For the two-regime model with a mean-reverting process for base regime (regime 1) and a Log-Normal distribution for the spike regime (regime 2) as defined in equations (2.25), the density functions of the two regimes used in (2.30) are as follows:

$$f(y_t|r_t = 1, \Omega_t; \theta) = \frac{1}{\sqrt{2\pi}\sigma_b} exp[-\frac{(x_t - x_{t-1} - \alpha(\mu_b - x_{t-1}))^2}{2\sigma_b^2}] \tag{2.32}$$

$$f(x_t|r_t = 2, \Omega_t; \theta) = exp\{\frac{1}{\sqrt{2\pi}\sigma_s} exp[-\frac{(TS - x_t - \mu_s)^2}{2\sigma_s^2}]\} \tag{2.33}$$

The density function of the shifted Log-Normal distribution is calculated similarly. The probability of being in a spike regime is set to zero for the prices under the threshold TS, and the probability of being in a drop regime is set to zero for the prices above the threshold TD.

2. Maximization step and iteration

   In the maximization step, the parameter set θ are estimated by maximizing the expectation of log-likelihood is calculated in the expectation step. The estimated parameters will be applied to the next expectation step to get an updated expectation of log-likelihood, and then maximization is implemented again. The two steps are iteratively implemented until the criteria of convergence is achieved.

2.4.2.4 Steady state probability of the regimes

The unconditional probability of being in one regime, which is the steady-state probability of the Markov chain, can be computed using the transition probabilities.For a Markov process with r states/regimes, the steady state probability can be calculated as follows [63]:

$$q * P = q \tag{2.34}$$

where, P is the transition probability matrix which is a $r \times r$ matrix. q is a $r \times 1$ row vector of steady state probabilities. The equation (2.34) can be solved together with the property of matrix P that the summation of each row equals to 1.

For a two-regime model, the unconditional probability of being in regime 1 is:

$$Prob(1) = \frac{(1 - p_{22})}{2 - p_{11} - p_{22}} \tag{2.35}$$

and the unconditional probability of being in regime 2 is:

$$Prob(2) = \frac{(1 - p_{11})}{2 - p_{11} - p_{22}} \tag{2.36}$$

2.5 Summary

In this chapter, the background material on primary methods, algorithms, and models were introduced in detail. Following the structure of this thesis, the methods studying the statistical characteristics were introduced. The calculation of two variability indices, historical volatility index and price velocity, were presented. The two classes of indices focus on different aspects of the fluctuation in time series, and thus are both applied to study the variability of reserve and regulation prices in Chapter 3.

The modelling of price dynamics decomposes the price time series into a deterministic component and a stochastic component. The procedures of this decomposition were presented in Section 2.3. After the deterministic component is removed from the prices, which comprises seasonality and a long-term evolution trend, the stochastic component is the main focus of price dynamics modelling.

Two popular classes of stochastic models used to study the price dynamics, the mean-reverting jump-diffusion and Markov regime-switching models, were presented in Section 2.4.1 and 2.4.2, respectively. The specific models in these two classes are selected based on the characteristics of prices in electricity markets. Both the two classes of models are capable of capturing the mean-reverting and jumps or spikes in the price processes, which have been widely observed in electricity energy prices. The two classes of models are applied to the reserve and regulation prices in this thesis to find the more appropriate model for these prices.

The two classes of models have similarities but are also different in nature. The MRJD model represents the jumps as a separate component. As MRS model has a latent regime/state variable R, the MLE method cannot be directly applied. An expectation-maximization (EM) method is used to estimate model parameters including the transition probabilities between regimes. In the expectation step, the likelihood function is calculated as the expected value considering the probability of being in a regime and the corresponding conditional density function. In the maximization step, the MLE is applied to estimate an updated set of parameters. The expectation and maximization steps are conducted iteratively to calibrate the model and estimate the parameters.

In addition, calculation of the steady state probability of a Markov chain was presented in Section 2.4.2.4. The steady state probability is an important indicator of the performance of the MRS model to identify excited regimes, such as spikes or drops. The calculation of steady state probability will be applied in Chapter 4 and Chapter 5.

The models introduced in this chapter, i.e., the MRJD model with independent jump component, the two-regime MRS model with shifted spike regime, and the three-regime MRS model with shifted spike and drop regimes, are applied to the studied prices in this thesis.

Chapter 3

Statistical Characteristics of the Reserve and Regulation Prices in the Electricity Market [1]

3.1 Introduction

The focus of this chapter is on analyzing the statistical characteristics of prices of operating reserves and regulation services in competitive electricity markets.

As reviewed in Chapter 1, statistical characteristics of energy prices in competitive electricity markets have been extensively studied in existing literature [23–25, 27–29]. However, not much attention has been paid to reserve and regulation prices. Characteristics of these prices are key to understanding the reserve and regulation markets. In this chapter, statistical characteristics of hourly reserve and regulation prices are explored for the electricity markets of Ontario, New York and Texas. Characteristics studied include descriptive statistics, price pattern, variability, price jumps and extreme prices, non-linearity and long-range correlations. The statistical characteristics of operating reserve and regulation prices in the Ontario and New York markets are compared with those of the energy prices in the respective markets.

The rest of this chapter is organized as follows. In Section 3.2, the studied markets and data are introduced. Descriptive statistics and the patterns of the studied data are analyzed in Section 3.3. In Section 3.4, characteristics of reserve and regulation prices, including variability, jumps and spikes, and long-range correlation are analyzed in detail and compared to those of the energy prices. Finally, a summary of the work and its main findings are provided in Section 3.5.

[1] Findings of this chapter have been published in *Energy Policy* [54].

3.2 The studied data

In this chapter, the available prices of energy, reserves and regulation services in the Ontario real-time market, the New York day-ahead market, and the day-ahead ancillary service market in Texas are studied and compared. The markets and prices are selected with consideration of the availability of information and the diversity of market structure. In the rest of this section, an introduction to the three markets and the studied data is given.

3.2.1 The Ontario market

Ontario's competitive electricity market opened on May 1, 2002. The Ontario market is a single-settlement real-time market where energy and operating reserves are jointly auctioned and prices are determined for each 5-minute operating interval. The energy/reserve co-optimization market program dispatches energy and reserve offers to minimize the total cost of supplying the demand. Since a generator can be scheduled to either produce energy or provide reserve, the optimization process was designed to find the most economical way to dispatch the offers. In particular, this process is explained for Ontario market in [4]. The hourly averages of 5-minute prices are used for most market settlements in Ontario.

Three classes of operating reserves are traded in Ontario's electricity market, namely, 10-minute spinning, 10-minute non-spinning, and 30-minute operating reserves. The total operating reserve requirement is defined as the largest capacity loss during a single contingency plus half of the capacity loss in the second largest single contingency. The total 10-minute reserve requirement is the capacity loss of the largest single contingency, and the 10-minute spinning reserve requirement is no less than 25% of the total 10-minute reserve requirement.

The hourly prices of operating reserves in the Ontario market are studied in the period of May 1, 2002 to December 31, 2007. The Hourly Ontario Energy Prices (HOEPs) for the same period are also studied for comparison purposes. The prices for the 10-minute spinning reserve, 10-minute non-spinning reserve and 30-minute operating reserve are denoted as ONR10s, ONR10n and ONR30, respectively.

Over the period of May, 2002 to December, 2007, the historical mean and maximum requirements for Ontario are as follows: 238.4 MW, and 450 MW, respectively, for the 10-minute spinning reserve; 683.9 MW and 1,570 MW, respectively, for the 10-minute non-spinning reserve; and, 472.9 MW and 855 MW, respectively, for the 30-minute non-spinning reserve. The administrative lower and upper price limits of the Ontario electricity market are -$2,000/MWh and $2,000/MWh, for both energy and reserves [3]. Currently there is no market for regulation service in Ontario.

The total generation capacity in the Ontario market was around 30,000 MW at the end of the studied period, i.e., year 2007. About 37.2% of the capacity came from nuclear power, 25.6% from hydro and other renewable resources, and 37.2% from thermal resources including coal, gas and oil, [4]. The peak load was 27,375 MW for the studied period.

3.2.2 The New York market

In the New York electricity market, operating reserves and frequency regulation service are procured in day-ahead and real-time [64]. However, the reserves are procured through a competitive market only in day-ahead. In real-time, the reserves are procured based on occasional needs. In addition, most of the energy demand is procured through the day-ahead market. Hence, only day-ahead prices are considered in this study.

The three classes of operating reserves are defined in the New York market similar to those of Ontario's market. The reserve requirements in the New York market are determined based on the capacity loss of the largest contingency, with details given in [65]. There are three reserve regions in the New York market, namely, East, West, and Long

Island regions. Locational requirements and prices are determined for each class of reserve in each region. Regulation service requirement is not locational, and suppliers are responsible for both regulation up and down services in the whole market. In the New York day-ahead market, energy, regulation and operating reserves are co-optimized to meet the corresponding demands at the lowest cost.

The historical prices in the New York market are analyzed in the period of February 5, 2005 to December 31, 2008. Based on our analysis, the historical prices for the East and West reserve regions behaved effectively the same. Thus, results are presented only for the East region. The 10-minute spinning reserve, 10-minute non-spinning reserve and 30-minute reserve prices are denoted as NYR10s, NYR10n, NYR30 respectively, while the regulation price is denoted as NYReg. The energy prices in the New York day-ahead market are also studied for comparison purpose. Several locational zonal energy prices are analyzed and their statistical characteristics are effectively the same when compared to the reserve and regulation prices. Hence, only the results for the price of Zone 6 are presented, i.e., the Hudson Valley area in the east of the New York state, as a representative price. This price is denoted as LBMP6.

The total generation capacity in the New York market was around 38,000 MW in 2008, with thermal resources making about 70% of the total capacity. About 14% of the total capacity was nuclear and the rest were hydro, wind and other resources [64]. The peak load in the New York market was 33,939 MW.

3.2.3 ERCOT market

The ERCOT operates the electricity market in Texas, United States. In the ERCOT market, most energy demand is satisfied by bilateral contracts and only less than 10% of energy demand is procured in the spot market [66]. Reserve and regulation services are scheduled in a day-ahead market. Compared to New York where the market is cleared for an entire day, the day-ahead ERCOT market is cleared for each single hour. In the ERCOT market, energy and reserves are procured separately, as opposed to the joint market optimization in Ontario and New York. In this chapter, the regulation and operating reserve prices from the ERCOT day-ahead ancillary service market are studied.

The operating reserves in the ERCOT day-ahead ancillary service market consist of responsive reserve and non-spinning reserve. The responsive reserve is similar to the 10-minute spinning reserves in the Ontario and New York markets, and it is required to be available in a few minutes. The non-spinning reserve needs to be available within 30 minutes when they are called. In normal conditions, the requirement for the responsive reserve is set at 2,300 MW to recover the capacity loss of failures of the two largest units. This requirement can be increased by up to 500 MW according to the system operating conditions. Regulation service in this market consists of regulation up and regulation down services.

The level of required regulation services in the past determines the requirements of regulation services. The amount of non-spinning reserve service plus the average regulation up amount need to be larger than 95% of the uncertainties observed in the load forecast accuracy evaluation. Uncertainty of wind power generation was added to this requirement in November, 2008 [66]. The required amount of regulation services were determined for blocks of several hours before year 2007; however, it is determined on an hourly basis after 2007.

In the ERCOT day-ahead ancillary service market, the responsive reserve and regulation up are cleared together because they both provide quick responding ramp-up capacity. The non-spinning reserve and regulation down are cleared simply based on the lowest-priced available offers that can meet the corresponding requirements.

The non-spinning reserve price is non-zero only when this reserve is procured. Until November 2008, the non-spinning reserve was procured in less than 25% of hours. However, this has increased to all hours since then [66]. Due to the large amount of zero prices, the non-spinning reserve price was not included in this study.

In the following sections, prices of responsive reserve, regulation up and regulation down are denoted by ERCOTRR, ERCOTRU and ERCOTRD, respectively. The studied prices are for the period of January 1, 2005 to December 31, 2009.

In the ERCOT market, the installed capacity of generation in 2009 was around 84,000 MW where more than 80% were gas- and coal-fired. Nuclear, wind, hydro, biomass, and other resources made the rest of the installed generation portfolio [66]. The peak load was 63,453 MW in the studied period.

3.3 Descriptive statistics and patterns of the studied data

To illustrate and understand the statistical characteristics of the studied prices, in this section the basic descriptive statistics are calculated for these prices. Differences in these statistics are observed between energy prices and the reserve and regulation prices, as well as among the markets. Fluctuation patterns in the studied prices are also investigated and the origins of the patterns are discussed.

3.3.1 Descriptive statistics

In this subsection, a set of descriptive statistics are calculated for the studied prices. More specifically, mean, standard deviation (STD), median, mode, max, skewness, and kurtosis are calculated for the energy, reserve and regulation prices in the studied markets. These statistics are shown in Table 3.1. The Ontario prices are in Canadian dollars, and the prices in the New York and ERCOT markets are in US dollars, but both dollars are represented as '$' for simplicity in presentation.

The descriptive statistics show substantial differences among the studied prices. Observe that the reserve and regulation prices are generally much lower than the energy prices,

Table 3.1: Descriptive statistics of prices in the studied markets ($/MWh)

	Mean	STD	Median	Mode	Max	Skewness	Kurtosis
HOEP	53.18	33.48	44.54	13.72	1028.40	5.09	76.72
ONR10s	4.87	10.94	3.17	0.20	660.01	25.64	1148.6
ONR10n	2.81	10.11	0.28	0.20	646.36	25.51	1173.7
ONR30	2.53	8.50	0.26	0.20	478.50	22.17	911.42
LBMP6	75.17	28.98	70.87	65.00	430.74	1.69	10.18
NYR10s	8.27	8.82	7.00	7.00	171.27	2.39	14.84
NYR10n	2.55	3.08	2.93	0.25	171.27	16.17	626.68
NYR30	0.79	1.11	0.50	0.50	36.74	6.09	123.02
NYReg	52.03	25.08	45.00	43.00	300.00	3.25	26.21
ERCOTRR	15.84	22.70	10.24	5.00	2000.02	35.20	2765.95
ERCOTRU	15.87	17.45	10.69	5.00	500.03	5.77	84.70
ERCOTRD	12.52	16.47	9.00	3.00	700.00	15.65	475.89

while the regulation and spinning reserves have higher prices than the non-spinning ones. The difference in price levels reflects the different costs of providing these products and services. The energy prices must reflect the production cost and thus they are high. The generally lower reserve prices are due to the fact that they are the payments for the capacity, and the costs of providing these capacity are much lower than producing energy. The cost of provision of spinning reserve is higher than the non-spinning reserve because generators may need to be activated or started up to be ready to provide these services [3], and this applies to regulation services as well. Moreover, the regulation service providers need to frequently change their operating positions, which can incur extra cost, and generators may be operating at a less efficient and less economical state when providing regulation and spinning reserve [66]. These extra costs will finally be reflected in their prices. Also observe that the reserve and regulation prices are more dispersive according to the high-order moments and the mode, median, and maximum. The substantially greater dispersion indicates more frequent and extreme values in these prices, forming a distribution with a longer right tail. The dispersion issues will be considered in detail in Section 3.4.

Obvious differences can also be observed between the markets. First, the Ontario market features the lowest energy and two reserve prices among the three markets, after the currency conversion. By converting the Ontario prices from Canadian dollar to US dollar based on annual exchange rates, the mean of the HOEP, ONR10s, ONR10n, ONR30 are 42.53, 3.77, 2.15, 1.95 US$/MWh, respectively. Observe that the first three are lower than the corresponding prices in the other two studied markets. This is partly due to the larger share of nuclear and hydro generation in Ontario's installed capacity [3]. Second, the regulation price in the New York market is greater than the regulation prices in the ERCOT market. The regulation service in the New York market includes both up and down services and thus has higher prices. Moreover, providing capacity for ramping up and down services simultaneously puts extra limits on the regulation suppliers when they set their operating points, which can be reflected in higher regulation prices [67]. Third, the responsive reserve price in the ERCOT market is much higher than the prices of 10-minute reserves in the other two markets. The differences between the characteristics of reserve price in the ERCOT and those of the other two markets arise from the differences in market design and structure for ERCOT. For example, unlike the other two markets, most of the energy demand in the ERCOT market is procured by bilateral contracts, and only a small portion of the demand is procured from the pool. Furthermore, the ancillary service market in ERCOT is a day-ahead market, and is separate from the energy market. However, in the New York and Ontario markets, the energy and reserve markets are dispatched jointly. In addition, as discussed in Section 3.2.3, ERCOT market is dispatched by minimizing the cost of operation over of each single hour, rather than all hours of the dispatch day. In general, this results in a less efficient scheduling and may result in a higher price level [66].

In order to analyze of the correlation between the statistical characteristics of the studied prices and load levels, the hourly prices are grouped with respect to their corresponding load levels, and the descriptive statistics are calculated for the groups. There is more than one possible way to break the data into different load categories. One way is to define a number of load thresholds and categorize hourly load values according to the thresholds. For example, by defining two load thresholds L1 and L2, three load categories can be defined. If the load is less than L1 at a certain hour, that hour is classified as low demand hour. If the load is between L1 and L2, the corresponding hours fall into the intermediate load level. Finally, if the loads at certain hours are more than L2, those hours are categorized as high demand hours. The drawback of this approach in the context of my analysis is that the continuity of the categorized load values may not be maintained. Another approach is to break the 24 hours of each day into a number of categories. For example, one may define certain hours of a day as low load level, some as intermediate load level and some as high demand hours. This approach is popular among utilities (e.g., [68–70]) and has the advantage of maintaining continuity of the categorized load time series. Thus this approach is selected here. The 24 hours of each day are divided into three 8-hour categories, as follows. The average load level for each of the 24 hours of the day is first calculated (e.g., for 10 a.m., the average is calculated over all loads at hour 10 a.m. for the entire study period). The 24 average loads are then sorted in ascending order. The first eight hours feature the lowest average loads, and are marked as low-load hours. The next 8 hours are marked as intermediate-load hours, and the remaining eight hours with the highest average loads are marked high-load hours. The 8 hours in each category identified by the above method are not necessarily consecutive hours of the day. For each day, the average of prices are calculated for the eight low-load hours, the eight intermediate-load hours and the eight high-load hours. Thus, each hourly price time series is converted into three new daily time series for the average prices of low-, intermediate- and high-load hours.

For each of the three time series, the descriptive statistics are calculated. Only the results for the Ontario market are presented in Table 3.2 for brevity; the results for the other two markets showed similar characteristics. The descriptive statistics from Table 3.2

Table 3.2: Descriptive statistics of prices with respect to load levels in the Ontario market ($/MWh)

	Low	Intermediate	High	Low	Intermediate	High
Price		HOEP			ONR10s	
Mean	36.3000	57.7545	65.4718	3.2298	4.6677	6.7204
Std	14.9387	24.4170	29.0337	1.6588	6.9059	7.2149
Median	34.0813	53.0150	60.0288	3.2963	3.1875	4.9513
Mode	38.5950	79.0188	91.6175	3.9300	0.2000	0.2000
Max	185.9225	301.9175	357.4800	17.0200	156.9950	81.323
Skewness	2.6913	2.3999	2.7363	1.0865	10.0072	3.0541
Kurtosis	18.6757	14.6647	18.1426	8.9387	170.9546	19.2605
Price		ONR10n			ONR30	
Mean	0.4537	2.8280	5.1382	0.4475	2.5759	4.5600
Std	0.6094	6.2925	6.9274	0.6008	4.9880	6.1081
Median	0.2000	0.7563	2.6975	0.2000	0.7038	2.5238
Mode	0.2000	0.2000	0.2000	0.2000	0.2000	0.2000
Max	7.6963	148.3775	74.9563	7.5113	108.9788	74.3438
Skewness	4.8243	10.7736	3.0366	4.8505	7.7751	3.3287
Kurtosis	35.1674	199.0021	18.0586	35.2954	124.2492	22.9796

show that the reserve prices are affected by the energy demand. All the reserve prices tend to have higher mean and dispersion when the load level increases. This trend holds in the other two markets as well. It is worth noting that the maximal reserve prices of the intermediate load group are higher than those of the high load group. This indicates that the reserve prices are not solely driven by the high demand for energy. More discussion on this issue is presented in Section 3.4.2.2. On the other hand, it can be observed that for the low-load hours, the maximal price is still much lower than those of the intermediate- and high-load hours. This implies that energy demand still affects the reserve prices.

Another observation is that, the skewness and kurtosis of the intermediate-load hours are higher than that of the high-load hours. This is because the high-load hours feature a high mean and thus, the extremely high prices have less impact on the overall price distribution.

It is also obvious that for any load level, the reserve and regulation prices still feature lower mean and higher dispersion, compared to energy prices, which are consistent with the statistics in Table 3.1.

3.3.2 Patterns of the studied prices

Sample plots of the reserves, regulation and energy prices for a typical one-week period are shown in Figure 3.1. For the Ontario and New York prices, the data are for January 15-21, 2007, and for ERCOT prices the data are for the week of August 11-17, 2008. The displayed prices represent the typical patterns in the studied prices.

From Figure 3.1, differences can be observed in the patterns of the reserve and regulation prices compared to the energy price. Generally speaking, all the studied reserve and regulation prices feature more frequent and substantial jumps. One important observation is that the reserve and regulation prices in the Ontario and New York markets tend to stay at low and nearly constant values for a few hours or longer before they burst into high levels. The ERCOTRR is smoother, but the fluctuation is still obviously larger than the energy prices in the other two markets.

Observe that similar to energy prices, the reserve and regulation prices are also determined by the supply and demand of reserve and regulation services. The main factors in the supply and demand characteristics that may contribute to this special pattern. First, the demand for reserve services usually remains constant until some step changes occur. The step changes result from the changes in system operation condition. Although the reserve requirements, i.e., reserve demands, vary in different markets, generally they are determined by the capacity of largest generation units or capacity loss in the most severe contingency events. Demand defined in this way is different in nature from the energy demand. The energy demand corresponds to the consumption of energy and continuously varies all the time. In contrast, the largest generation unit and most severe contingency usu-

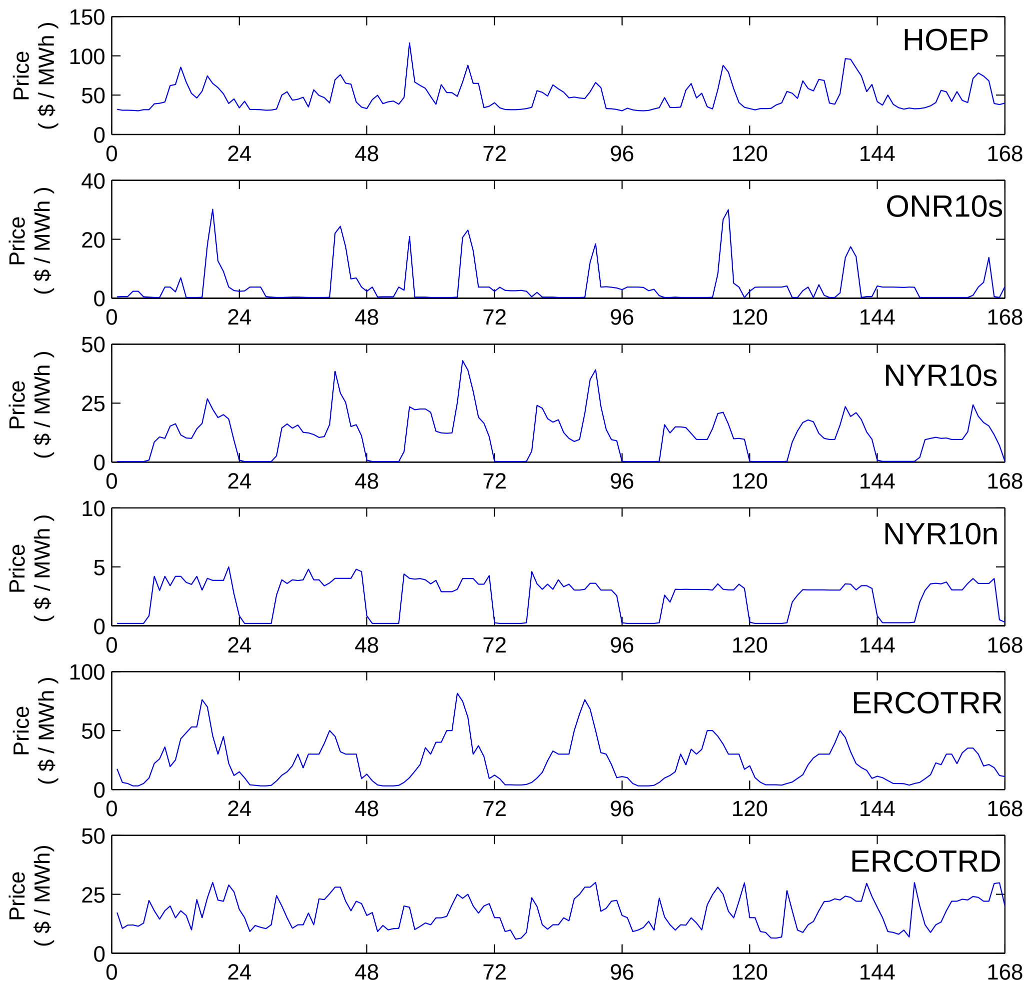

Figure 3.1: Price plots in typical one week window

ally remain the same until some non-frequent events occur, for example, planned or forced capacity reduction of generation units and transmission lines. The constant parts in the reserve demand can therefore explain the flat parts in reserve price plots. When the reserve requirements are revised due to the events mentioned above or the manual adjustment by the market operator, they usually change in a discrete way, thus leading the reserve price to exhibit sudden jumps.

Second, the demand for reserve and regulation services is much less than the energy demand. Thus, the change of a scheduled supply offer in the joint optimization procedure can have a large impact on the supply curve for reserve regulation, while it has a lesser impact on the energy supply curve.

Third, the supplies available in the reserve and regulation markets are affected by the energy market as well. The reserve and regulation suppliers would consider the opportunity cost when they bid. For example, when the energy price is expected to be high, the generation suppliers tend to participate in the energy market and raise their bid of reserve and regulation prices. The impact from the energy market implies that the energy demand can also affect the reserve prices, as shown in Table 3.2. This partly explains the existence of seasonality in the reserve and regulation prices. In fact, the seasonality of the reserve and regulation prices have been checked by the Power Spectral Density (PSD) method [28, 71]. The results for the Ontario 30-minute reserve price is presented in Figure 3.2 as an example. The highest peak occurs around the frequency of 0.042 which corresponds to a period of 24 hours, representing the daily seasonality. There are peaks around the frequencies of 0.083 and 0.125 which are 2 and 3 times of the daily frequency which is 0.042. Another peak appears around frequency of 0.006 which corresponds to the period of 168 hours, i.e., the weekly seasonality. In addition, the peaks close to zero correspond to the annual seasonality. The PSD analysis shows that the reserve and regulation prices also have daily, weekly, and annual seasonality which have previously been reported for energy prices [28, 31, 44].

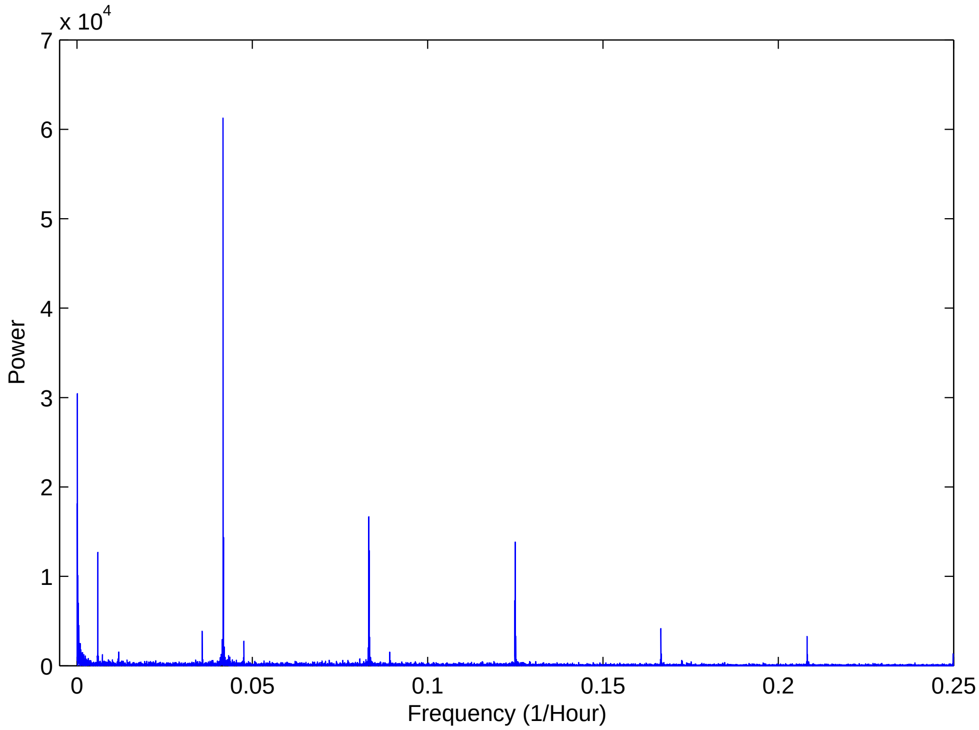

Figure 3.2: Power Spectral Density of the Ontario 30-minute operating reserve price

3.4 Characteristics of Reserve and Regulation Prices

Characteristics of the reserve and regulation prices are investigated in detail in this section. Variability, price jumps and extreme prices, long-range correlation and non-linearity properties are discussed. Comparisons with energy price behavior are made where possible.

3.4.1 Variability

Hour-by-hour electricity market price variability is mainly driven by the load level and the bid price of the marginal generator at each hour. Variability of electricity prices has been measured by historical volatility and price velocity indices [23–25]. Electricity prices have been reported to have higher variability than the prices in other markets such as, stock market prices [23]. Thus, high variability is a distinguishable characteristic of energy prices. In this subsection, the variability in reserve and regulation prices are specifically studied.

3.4.1.1 Relative Variation Index

As discussed in Chapter 2, historical volatility index (HVI) is calculated from price returns. However, the standard definition of the price returns cannot be directly used in this study because of the existence of zero prices. In the studied period, there are 83 zero prices out of 49,704 observations in the ONR30, 11 zero prices out of 34,224 observations in the NYR10s and NYR10n, and 1,082 zeros in the NYR30 price. Although not a very large portion of the entire price process, the zero prices cannot be simply removed from the sample because they are a part of the price processes. However, the zero prices limit the effective and reliable deployment of the traditional volatility index, which is computed based on the price returns.

To overcome this problem, the formula to compute the arithmetic return (2.2) is revised by replacing the dominator with the daily average. The revised return is called relative variation, and can be calculated as follows:

$$RV_l(t) = \frac{x(t) - x(t-l)}{\overline{x}^{(k)}} \tag{3.1}$$

where, $\overline{x}^{(k)}$ represents the daily average of hourly prices for day k. The relative variation calculates price changes with respect to the mean price in a day, while price return calculates price changes with respect to the price of a single hour. Thus, they both represent the variation in price with respect to its own level. Following the computation of historical volatility, in the next step the revised variation index is calculated based on the standard deviation of $RV_l(t)$. The revised form of the HVI is named Relative Variation Index (RVI). RVI is calculated as explained below. The standard deviation of RV over a time window is firstly calculated as:

$$\sigma_{l,T}(n) = \sqrt{\frac{\sum_{t=(n-1)\times T+1}^{n\times T}(RV_l(t) - \overline{RV}_{l,T}(n))^2}{T-1}} \tag{3.2}$$

where, $\sigma_{l,T}(n)$ is the standard deviation of RV in the n^{th} time window based on two parameters, i.e., the time lag l and the time window length T. $\overline{RV}_{l,T}(n)$ is the average of $RV(t,l)$ in window n. The standard deviations $\sigma_{l,T}(n)$, whose average is the RVI$_l$, are calculated for windows of T hours. The index RVI$_l$ basically follows the definition of the HVI, but based on relative variation which is a revised form of price return, both of which represent variability of prices.

Following the work in [23, 25], window length $T = 24$ is chosen for the present study. In [25], the historical volatility index has been extended with different values of l. The three cases l=1, 24, 168 used in [25] corresponds to intraday, inter-day, and inter-week volatilities, respectively. These three cases are also chosen for RVI. The numerical results are given later in this section.

3.4.1.2 Comparison of variability

The two classes of variability indices, i.e., the RVI proposed above and price velocity indicies intorduced in Chapter 2, focus on different aspects of the variability. The price velocity indices represent the relative absolute changes in prices with respect to the average price, while the RVI represents the variation of the relative price changes. Both of these two classes of variability indices are presented in this study in order to draw a more reliable conclusion. Observe that standard deviation of prices quantify the variations of price over a long period of time. However, price velocity indices quantify relative price fluctuations, and the RVI quantifies the standard deviation of relative price fluctuations.

The RVI and price velocity index $\overline{\text{DVDA}}$ are calculated for the studied prices. The values of the indices are shown in Table 3.3 compared between the energy prices and the reserve and regulation prices in the rest of this section. In the two price velocity indices

DVDA and DVOA, only the DVDA index is presented here because the results of the two indices were found to be consistent for the studied prices.

Table 3.3: Variability of the prices in the studied markets

	RVI_l			$\overline{\mathrm{DVDA}_l}$		
l	1	24	168	1	24	168
HOEP	0.2812	0.3828	0.4059	0.1778	0.3036	0.3760
ONR10s	1.0441	1.5473	1.9003	0.5058	0.8369	1.1005
ONR10n	1.3980	3.3923	3.8706	0.5566	1.3233	1.6341
ONR30	1.3844	3.2595	3.9201	0.5527	1.2858	1.6552
LBMP6	0.1083	0.0837	0.0967	0.0780	0.0995	0.1614
NYR10s	0.5051	0.4982	0.5813	0.2775	0.3509	0.4279
NYR10n	0.6264	0.5830	0.7424	0.3555	0.3555	0.5027
NYR30	0.5705	0.7062	0.8358	0.4327	0.4327	0.5608
NYReg	0.2498	0.2491	0.2655	0.1191	0.1458	0.1664
ERCOTRR	0.5190	0. 5062	0.6715	0.3236	0.3679	0.5517
ERCOTRU	0.6017	0.4386	0.6263	0.3750	0.2971	0.4703
ERCOTRD	0.5991	0.3956	0.5374	0.3593	0.2528	0.3944

Significantly greater variability can be observed in the reserve and regulation prices compared to the energy prices in each of the Ontario and New York markets. This observation is consistent according to the two employed variability indices and all three time scales. The higher levels of these indices indicate that both the relative price changes and the variation of relative price changes are higher for the reserve and regulation prices compared to energy prices. Note that volatility of the Ontario energy prices are previously reported to be highest among the other North American electricity market prices [25]. However, the studied reserve and regulation prices are, in general, significantly more volatile/variable than the Ontario energy prices. Another comparison has been made between the price velocity indices in Table 3.3 and the ones calculated in [24] for energy prices in fourteen electricity markets. It can also be observed that the variability of all the studied reserve and regulation prices expect NYReg is significantly higher.

Note that the relatively frequent jumps along with the generally lower prices, compared to the energy price, which can be observed in Table 3.1 and Figure 3.1, result in the higher variability indices. In most of the days, a period of flat prices is usually followed by a jump. This results in sharp changes in price variations and subsequently larger RVI values. As discussed in Section 3.3.1, the relatively lower prices for the reserve and regulation services are because of the lower cost of providing these services. Also, as discussed in Section 3.3.2, the frequent jumps in the reserve and regulation prices are partly caused by the step-changing nature of the demand for these services.

In [30], the daily tertiary reserve prices in the German market showed lower volatility than the energy price. The large difference arises from the different market designs. Note that hourly prices are studied in this chapter. Hourly uniform clearing prices are determined based on the highest scheduled bid. On the other hand, the German tertiary reserve market is a pay-as-bid market where suppliers are not paid by a uniform clearing price. The tertiary reserve offers were cleared in blocks of hours and the price of each block is the weighted average of all cleared offers. The daily tertiary reserve prices studied in [30] is the sum of all block prices of a day [72]. The difference between the results of [30] and those presented in this chapter may also attribute to the variation of generation resource used to provide the tertiary reserve in the German market, compared to those markets studied here.

Comparing among the three markets, the Ontario market features the highest variability level in energy and reserve prices. One reason contributing to this higher variability level in the Ontario market originates from the market mechanism. As introduced in Section 3.2, the Ontario market is a single-settlement real-time market, and thus, only real-time prices are available. For New York market, the reserves are procured through a competitive market only in day-ahead, and in the ERCOT market, there is only a day-ahead market for the studied reserve and regulation prices. Hence in these two markets, only day-ahead prices are studied. The higher price variability in the Ontario market, compared to the day-ahead New York and ERCOT markets, is a direct result of the real-time scheduling in Ontario [25].

The variability of prices corresponding to the three load levels, i.e., low, intermediate and high, are also studied here. The methodology of converting the hourly prices into the average daily prices is presented in detail in Section 3.3.1.

For each of the three time series, the variability is calculated. Only the results of RVI for the Ontario market have been presented in Table 3.4, but the price velocity and variability indices for the other two markets are also discussed. The values of time lag l in (3.1) and (3.2) for this case are $l = 1$ and $l = 7$ correspond to daily and weekly price variations.

The general observation is that all the variability indices are lower for the low-load hours compared to the other two load levels. For reserve prices, the intermediate-load hours generally feature higher variability than the high-load groups. The reason is that the intermediate-load group has a lower mean and extreme prices start to take place in this group; thus, the relative price changes can be high. In all the markets it can be observed that the reserve and regulation prices still feature higher variability compared to energy prices, in each load level.

Table 3.4: RVI of the prices with respect to load levels in the Ontario market

	Low	Intermediate	High	Low	Intermediate	High
Price	HOEP			ONR10s		
l=1	0.2424	0.3089	0.3176	0.3419	0.9318	0.8677
l=7	0.2825	0.3279	0.3509	0.3915	1.0032	0.9318
Price	ONR10n			ONR30		
l=1	0.4085	1.2336	1.0157	0.4139	1.1192	1.0220
l=7	0.4993	1.3088	1.0836	0.4985	1.1857	1.1075

3.4.1.3 Clustering of variability

Clustering of variability is a characteristic that the variability is greater during certain hours of the day than the other hours. This characteristic is explored in this section for the studied prices following the approach in [23, 25]. The clustered high levels of variability was observed by a sensitivity study of the variability index HVI with respect to the hour of the day in [23, 25]. Following Section 3.4.1.1, the revised form of HVI, i.e., the RVI index, is used for the variability sensitivity study. First, price time series x is divided into 24 sub-series, each sub-series x_i containing the prices of hour i. The relative variation is calculated for each sub-series x_i as in (3.1). Here, the lag parameter $l = 1$ is picked to calculate the relative variation between adjacent days. The standard deviation of relative variabilities for each sub-series is then calculated based on (3.2) for seven-day time windows. The RVI values for each hour are plotted in Figure 3.3.

From Figure 3.3, clustering property has been shown in the variability of all the studied prices, but with different patterns. For all the energy and reserve prices in the three markets plus the regulation up price in the ERCOT market, the RVI values are relatively high from early morning until late evening. These hours are mainly the on-peak hours featuring high energy demand and price. In these on-peak hours, the availability of generators to provide ramping-up capacity is reduced because of the high energy demand. Operating reserves and the regulation up service, both of which supply ramping-up capacity, also feature high prices in these hours as a result of less available supplies for the ramping-up capacity and higher opportunity cost of supplying this kind of capacity. Day to day price changes in these high-price hours may vary a lot because the market clearing point is pushed toward the steep part of the supply stack curve by the higher demand in these hours. In such case, the RVI tends to be high because it is defined as the standard deviation of price changes.

The regulation down price in the ERCOT market, ERCOTRD, has relatively high variability from the midnight until early morning and relatively low variability in the other

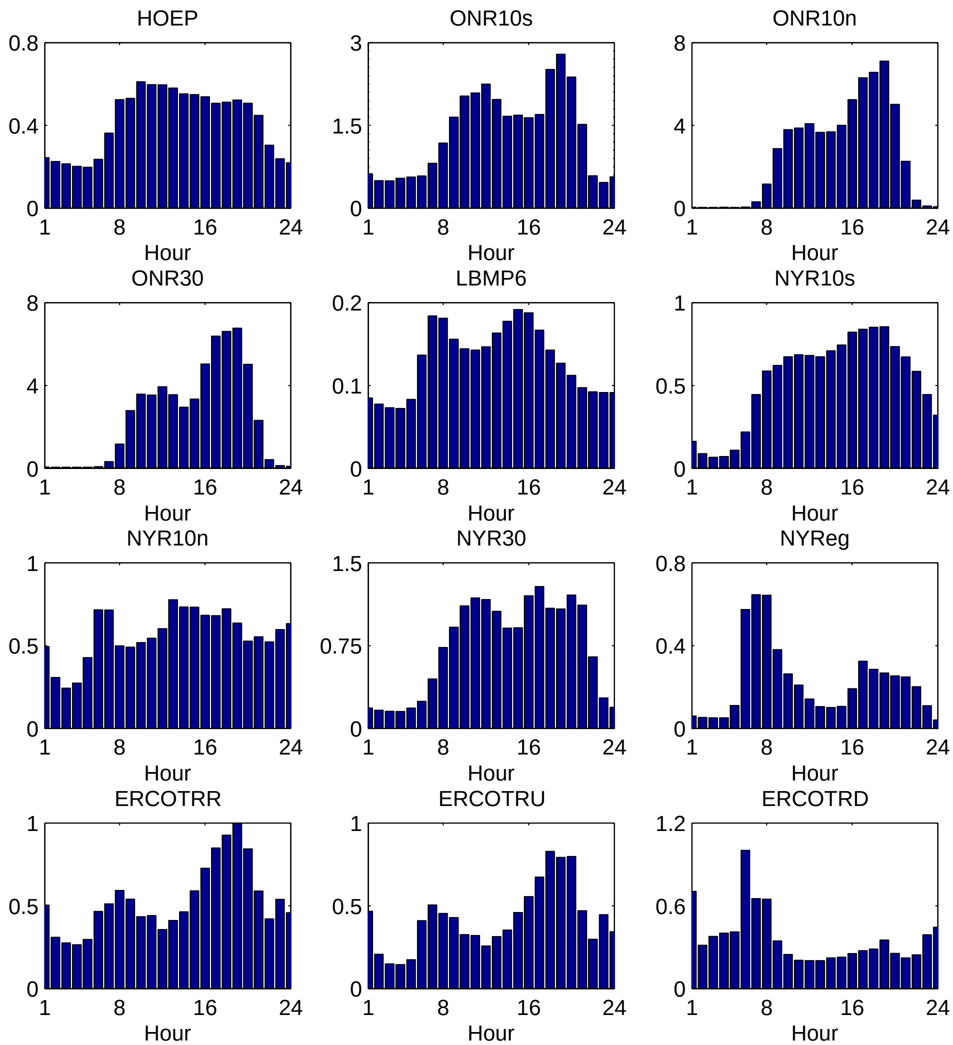

Figure 3.3: Volatility of hour-of-the-day in the studied markets

hours. The reason is the lower available supply of this service in these hours. The energy demand is generally less from midnight until early morning. The low energy demand requires less on-line generation capacity and thus the available ramping-down capacity is lower than the on-peak hours [66]. In addition, during those hours, only baseload units are normally available. Those units, however, are not well suited for providing fast ramping services. Similar to the discussion in the previous paragraph on the high ramping-up capacity price and variability, the tight supply condition of the ramping-down capacity results in high regulation down price with high variability. The regulation service in the New York market accounts for both regulation up and down services. Thus, its price has a peak in the morning hours as well as another peak in the late afternoon and early evening hours, which are basically the ramping hours.

All the reserve and regulation prices appear to have a more pronounced variation in their variability compared to the energy prices. This is generally due to their lower price levels and higher sensitivity to changes in the market.

3.4.2 Jumps and extreme prices

A well-known characteristic of energy price is the sudden and extreme price changes in the short time. The values of skewness and kurtosis in Table. 3.1 show that distributions of the reserve and regulation prices tend to have longer right tail than the energy prices, implying that more extreme prices exist in the reserve and regulation price processes, and the magnitude of the extreme prices are farther away from the mean of these prices. The existence of price jumps and spikes has been recognized as a result of the limited storability and demand elasticity in power systems [27]. The extreme price changes and the consequent high prices is a very important issue in energy price modelling and forecasting literature [26], [73, 74], and is the main source of inaccuracy of price models.

In this subsection, focuses are specifically put on two aspects of jumps. First, the fre-

Table 3.5: Price jump frequency for the studied prices

Price	f_{jump}	Price	f_{jump}	Price	f_{jump}
HOEP	0.0168	LBMP6	0.0129	ERCOTRR	0.0165
ONR10s	0.0251	NYR10s	0.0212	ERCOTRU	0.0182
ONR10n	0.0291	NYR10n	0.0155	ERCOTRD	0.0222
ONR30	0.0289	NYR30	0.0245		
		NYReg	0.0256		

quency of the price jumps are studied, second, it will be shown extreme prices for reserve and regulation do not necessarily coincide with high energy prices.

3.4.2.1 Price jumps

The jumps in prices are identified by the jump filtering algorithm introduced in Section 2.2.2. The jump frequencies are then calculated as the ratio between the number of jumps and number of observations in the price process, i.e., the length of the price time series. The jump frequencies of the studied prices are shown in Table 3.5.

From Table 3.5, the reserve and regulation prices tend to have more frequent jumps compared to energy prices in the Ontario and New York market, while in the ERCOT market the jump frequencies are lower but still significant. As analyzed in Section 3.3.2, the reserve requirements tend to have step changes and result in jumps in reserve prices. Furthermore, the discrete variation in reserve requirement may be relatively large when the system operating condition changes. For example, on September 7, 2003, the total operating reserve requirement in the Ontario market increased from 1,580MW to 2,350MW [3]. This increase was a result of an outage of a transmission line. During the outage, two nuclear units were connected to the system by a single transmission line, which increased the capacity loss of the largest single contingency and therefore the reserve requirement increased. Significant changes in reserve requirement, i.e. reserve demand, can therefore cause high reserve prices and form price jumps.

It is noticed that in each case the frequency is much higher than 0.0015, which is the probability of being outside the confidence interval of three standard deviations for observations drawn from a Normal distribution. This observation implies that the price changes of all the studied prices have a heavy right tail, while the reserve and regulation prices generally have a heavier right tail compared to the energy prices.

3.4.2.2 Occurrence of extreme prices

The objective of this section is to check if the extreme prices occur simultaneously in energy, reserve and regulation prices. In this study, extreme prices are defined as rarely occurred extremely high prices. Since the extreme prices do not tend to last for long time, they usually appear as price spikes. The ERCOT market is not included because its energy price is not studied in this work.

In the Ontario market, the threshold to detect extreme abnormal prices in the energy price is \$200/MWh in Canadian dollars. However, in the studied period, only 207 out of 49704 hours are extreme price hours, which is only 0.42% of the data. To better illustrate the characteristic of the occurrence of extreme prices, the threshold of identifying extreme prices is set to the 98% percentile of the studied prices. That being said, the highest 2% of prices are recognized as extreme prices in each studied price time series. For the prices studied in the Ontario market, the thresholds are at \$141.23, \$28.16, \$27, and \$24.72 CAD for HOEP, ONR10s, ONR10n, and ONR30, which are 266.6%, 587.2%, 960.1%, and 977.1% of their corresponding mean values, respectively.

The occurrence of extreme values in the studied prices are determined and compared for the Ontario and New York markets. It was found that, the occurrence time of extreme prices in the energy price and reserve prices are significantly different. The HOEP shared no more than 19% occurrence time with the reserve prices. The three types of reserve prices share more than 70% occurrence time with each other, that is, in 70% of the hours where there is an extreme price in one reserve price, prices also suffer extreme values in the other two classes of reserves. In the New York market, the extreme reserve prices coincide with extreme energy prices shares for about 20% of the hours, similar to that of the Ontario market.

One reason behind this difference may be that the supply bidding in the energy and reserve markets are different. Generation suppliers such as Hydro-electric in the Ontario market may bid a high price in the energy market while bidding a low price in the reserve market as a backup. Thus, in case the supplier is not scheduled in the energy market, the reserve market bidding can be scheduled and gain revenue [3]. Another reason lies in the difference of the energy and reserve demands. Take the Ontario example in Section 3.4.2.1 again, on September 7, 2003, the reserve demand was raised significantly and as a result the reserve price reached extreme value. However, in these hours the energy price was normal because the energy supply and demand were basically not affected [3]. The different impacts on energy and reserve prices are due to the fact that energy price is determined by energy demand and available generation capacity at the current moment, but the reserve requirement, and thus the reserve price, is affected by the capacity loss caused by possible future contingencies.

However, observe that since the extreme prices are defined as the top 2% of prices, the above analysis is only focusing on these rarely appeared high prices. As observed in the price plots, the reserve and regulation prices mainly follow the up and down trend of the energy prices in an overall sense, driven by the marginal unit providing the last MWh of generation at that time. Factors that are driving forces of energy prices, including fuel price, demand and unexpected contingencies in the energy market, would generally affect the regulation and reserve prices as well.

3.4.3 Long-range correlation and non-linearity

The detrended fluctuation analysis (DFA) introduced in Chapter 2 is applied to the studied prices. The generalized Hurst exponent $H_{p,q}$ for the studied markets are shown in Table 3.6 with $p = 1$ and $q = 2$ which is the standard form of DFA. The number of significant digits is selected based on the scale of the presented values. It has been observed that the slopes (the values of $H_{p,q}$) are different for the electric energy price with time scales that are shorter than one day (i.e. intraday) and longer than one day (i.e. inter-day) [29]. Thus, the $H_{p,q}$ of intraday and inter-day time scales are computed separately since there is a pronounced difference between them in all studied prices. Generally speaking, in this table, the scaling exponents are all greater than 0.5 and smaller than 1.5, indicating the existence of persistence as well as randomness in the studied prices. In previous research, the Hurst exponents obtained for the energy price returns were less than 0.5, indicating a mean-reverting property in the energy price because a drop trend tends to occur after a positive price change [28]. However, in this study the $H_{p,q}$ for price itself, rather than price change, is calculated. In this case, the Hurst exponent less than 1.5 is consistent with the cases where the Hurst exponent is less than 0.5 for price change [29].

The reserve and regulation prices basically have smaller $H_{p,q}$ compared to energy price in the studied markets, and are smaller than the $H_{p,q}$ of the energy prices shown in [29]. Although smaller than the energy price, the $H_{p,q}$ of reserve prices are also significantly greater than 0.5, which indicate that they are predictable, since the values in the future are not totally random, i.e. they are correlated to the past prices. On the other hand, the smaller $H_{p,q}$ compared to the energy prices imply that the reserve and regulation prices are more difficult to predict. The low predictability also relates to the greater dispersion in heat-rates and variable generation costs in those units supplying the reserve and regulation services. Besides, the $H_{p,q}$ of both energy and reserve prices are generally higher in the New York market compared to the Ontario market, implying the better predictability in the

Table 3.6: $H_{p,q}$ in the studied markets

Price	HEOP	ONR10s	ONR10n	ONR30
Intraday	1.1088	0.7601	0.7944	0.8180
Inter-day	0.9172	0.8288	0.8457	0.8771
ρ_{DFA}	0.2995	0.5810	0.8881	0.8390
Price	LBMP6	NYR10s	NYR10n	NYR30
Intraday	1.4309	1.2457	1.3234	1.1376
Inter-day	1.0588	0.9542	0.8975	0.9422
ρ_{DFA}	0.1720	0.2269	0.5591	0.5418
Price	NYReg	ERCOTRR	ERCOTRU	ERCOTRD
Intraday	0.8890	1.1330	1.1472	0.7724
Inter-day	0.9692	0.7800	0.8107	0.8508
ρ_{DFA}	0.3597	0.5555	0.3610	0.5191

day-ahead market. Moreover, the intraday and inter-day Hurst exponents are different for all the studied prices, indicating different dynamics in these prices in intraday and inter-day time scales [29].

The DFA analysis can be extended to measure the non-linearity of a time series. When multifractility (non-linearity) exists in the studied time series, the $H_{p,q}$ computed from the DFA will be sensitive to the norm parameter q. Thus, non-linearity can be detected from the DFA analysis. The sensitivity of $H_{p,q}$ with respect to q has been used in [29] to detect the non-linearity of a price time series. The non-linearity index is computed as $\rho_{DFA} = H_{q_{max}} - H_{q_{min}}$. This represents the difference in scaling behaviors of the segments with fluctuations of different scales [58].

In Table 3.6, the sensitivities are studied for the Ontario and New York market prices. In the present work, q_{min}=0.1 and q_{max}=20 are picked following [29]. The results shown in this Table 3.6 indicate that all the studied prices are non-linear. From the table, the sensitivity is obviously more substantial in most studied reserve and regulation prices, demonstrating greater multifractality or non-linearity in these prices. This observation is not surprising after the high variability as well as the frequent and severe jumps are detected in these prices. The results in Table 3.6 imply that linear time-series models are less adequate and non-linear models are preferred for modelling and forecasting reserve and regulation prices.

3.5 Conclusion

In this chapter, various statistical measures have been implemented to investigate the characteristics of reserve and regulation prices in three North American markets. Particularly, price variability has been analyzed using a variant of historical volatility and price velocity. Moreover, price jumps and extreme prices, long-range correlations and non-linearity have also been investigated. These characteristics have been compared with those of energy prices where possible.

In general, the studied reserve and regulation prices featured lower price levels, larger dispersion and different patterns compared to the energy prices. The variability was significantly higher in reserve and regulation prices compared to that of energy prices in all the studied time horizons, i.e., hourly, daily, and weekly variability. Also, a clustering property was observed for the studied prices, i.e., high variability tends to occur continuously over a certain period during a day. The observed variability implies that the changes in the power supply, including the hour-to-hour changes in costs of providing the energy and ancillary services, and availability of generators, have a significant effect on the prices of energy and ancillary services.

The descriptive statistics and variability studies have also been applied to reserve and regulation prices for low-, intermediate- and high-load hours. It was observed that the studied prices had greater mean, dispersion and variability during intermediate-load hours, compared to high-load hours. This observation indicates that while demand level influences the variability of prices, it is not the only factor in price variability of reserve and regulation services. Other factors, such as change in system operation conditions and the ability of the system to respond to those changes, also impact the variability of reserve and regulation prices.

It was also found that the studied reserve and regulation prices had more frequent jumps and extreme prices. Furthermore, jumps in the prices of reserve, regulation and energy markets did not necessarily occur at the same time. In addition, compared to energy prices, lower long-range correlation and higher non-linearity were detected in the reserve and regulation prices. It has also been observed that seasonal cycles and the positive auto-correlation exist in the reserve and regulation prices.

The statistical characteristics of the reserve and regulation prices were found to vary across the three studied markets. The observed differences are mostly driven by the structure and design of the markets. For example, the Ontario market features higher variability due to its real-time-only market settlement mechanism and relatively low prices partly due to the larger share of hydro and nuclear generation in Ontario. The regulation prices of New York and ERCOT markets have largely different mean levels because of the different definitions of regulation services in these two markets.

Generally speaking, the higher variability as well as the more frequent and substantial jumps in the reserve and regulation prices imply the greater difficulty in modelling and forecasting these prices compared to energy prices. This observed variability also implies that hour-to-hour changes in the fuel types, technologies and availabilities of the electric generators that set market prices for energy, reserves and regulation services have a significant effect on prices, which is difficult to capture in retrospective statistical analyses. Nevertheless, this study illuminates important differences in these prices in the three markets analyzed in this chapter. The findings in this chapter can provide useful information to market participants in their operation and planning. The characteristics of the reserve and regulation prices are helpful to building models for these prices, which are presented in Chapter 4 and Chapter 5.

Chapter 4

Modelling Reserve and Regulation Prices in Competitive Electricity Markets [1]

4.1 Introduction

Stochastic models are important tools for risk management and pricing of financial products. In this chapter, two classes of models, i.e., the mean-reverting jump-diffusion (MRJD) model and the Markov regime-switching (MRS) model, are selected for modelling reserve and regulation prices. Three models from these two classes, which have been found to be most effective in modelling prices with spikes and time-varying volatility, are applied to the daily average reserve and regulation prices. Performance of these stochastic models are compared to find the most appropriate model for these prices.

The rest of this chapter is organized as follows. In Section 4.2, the studied daily prices are introduced, and their descriptive statistics are discussed. Also, some descriptive statistics and the patterns of the studied data are analyzed in this section. The selection of models is presented in Section 4.3. In Section 4.4, the model simulation procedures are introduced and numerical results are discussed. The calibration results of the three selected models are displayed and analyzed in Section 4.5. The performance of the three models are compared in Section 4.6. Finally, a summary of the work and its main findings are provided in Section 4.7.

[1] Part of the findings of this chapter have been submitted to *IEEE Transactions on Smart Grid*

4.2 The studied data

In this chapter, descriptive stochastic models are fit to the prices of operating reserves and regulation service in the Ontario real-time market and New York day-ahead market. Models are also built for energy prices in the same markets for comparison purposes. The studied prices and their basic descriptive statistics are presented and analyzed in the rest of this section.

4.2.1 The data studied

The daily averages of reserve and regulation prices in the Ontario and New York electricity markets are studied in this chapter. In the Ontario market, the daily average prices of operating reserves is studied in the period of May 1, 2002 to December 31, 2007. The prices for the 10-minute spinning reserve, 10-minute non-spinning reserve and 30-minute operating reserve are denoted as ONR10s, ONR10n and ONR30, respectively. The energy price is denoted as DOEP, which stands for daily Ontario energy price.

In the New York market, models are applied to daily average prices in the time frame from February 5, 2005 to December 31, 2008. Following the work in Chapter 3, the prices studied include reserve prices in the East reserve region, regulation price, and energy price of zone 6. The 10-minute spinning reserve, 10-minute non-spinning reserve and 30-minute reserve prices are denoted as NYR10s, NYR10n, NYR30, respectively. The regulation price is denoted as NYReg, and the energy price of zone 6 is denoted as LBMP6.

4.2.2 Descriptive statistics of the studied data

The studied daily prices are the equally weighted averages of 24 hourly prices of each day. Daily prices have been examined in most of the existing literature that focused on modelling energy prices in electricity market, such as [26, 33, 34, 38–42]. Note that taking daily average will remove negative and zero prices and thus, the logarithmic transformation can be directly applied to the prices in model building stage.

Mean, standard deviation (STD), median, maximum, skewness and kurtosis of the daily energy, reserve and regulation prices in the studied markets are shown in Table 4.1. The statistics of the corresponding hourly prices are also presented for the convenience to compare them. The prices names in Table 4.1 that start with ”D” are daily prices, while the ones that start with ”H” are hourly prices. Sample plots of studied reserve prices are displayed in Figure 4.1, and Daily average Ontario energy prices (DOEP) are also shown for comparison purposes. The time frame of the sample plots for Ontario market is January 1 to December 31, 2003, and is January 1 to December 31, 2007 for the New York market. The prices are in Canadian dollars for the Ontario market and US dollars for the New York market. Both dollars are represented as $ for simplicity in presentation.

The statistics of the daily prices in Table 4.1 show consistencies with the statistics of the hourly prices. The mean levels of all the studied daily prices are the same as the corresponding hourly prices, because the daily prices are the equally-weighted averages from hourly prices. The differences between the daily energy prices and the daily prices of reserve and regulation services are consistent with those for the hourly prices. The reserve prices present greater dispersion, as their STD/mean ratios are generally higher than those of energy prices. Higher skewness and kurtosis values in reserve prices further demonstrate that the reserve prices are more dispersive than energy prices. Positive skewness values indicate that the distributions of the prices have longer right tails, which implies existence of high prices and spikes. It can also be observed from the sample plots in Figure 4.1 that the reserve prices feature more frequent and extreme spikes, while the energy price process is smoother. The maximum of the prices in Table 3.1 also confirm that reserve prices have more extreme spikes. For example, the maximum of ONR10s is 65.17 $/MWh which is over 17 times of its median, while the maximum of DOEP is 220.32 $/MWh, which is about 4.5 times of its median.

Table 4.1: Descriptive statistics of daily and hourly prices in the Ontario and New York markets (All prices with unit \$/MWh)

	Mean	STD	Median	Max	Skewness	Kurtosis
DOEP	53.18	20.87	49.32	220.32	2.08	11.05
HOEP	53.18	33.48	44.54	1028.40	5.09	76.72
DONR10s	4.87	4.34	3.74	65.17	3.82	33.02
HONR10s	4.87	10.94	3.17	660.01	25.64	1148.6
DONR10n	2.81	4.02	1.33	58.13	4.02	33.77
HONR10n	2.81	10.11	0.28	646.36	25.51	1173.7
DONR30	2.53	3.45	1.33	43.48	3.46	24.43
HONR30	2.53	8.50	0.26	478.50	22.17	911.42
DLBMP6	75.17	21.17	70.56	191.65	1.35	5.61
HLBMP6	75.17	28.98	70.87	430.74	1.69	10.18
DNYR10s	8.27	4.75	6.85	38.80	2.14	8.41
HNYR10s	8.27	8.82	7.00	171.27	2.39	14.84
DNYR10n	2.55	1.73	2.34	34.59	6.83	110.05
HNYR10n	2.55	3.08	2.93	171.27	16.17	626.68
DNYReg	52.03	14.80	52.17	119.73	0.15	4.49
HNYReg	52.03	25.08	45.00	300.00	3.25	26.21

On the other hand, the statistics in Table 4.1 show differences between daily and hourly prices. The dispersion in the daily prices are generally lower than these of the hourly prices, demonstrated by smaller standard deviation, maximum, skewness and kurtosis. Therefore, the daily prices are smoother compared to hourly prices. This is as expected because the hourly high and low prices in the same day will offset each other when daily average is taken.

4.3 Selection of models

In this chapter, three models that have been introduced in Chapter 2 are applied to the studied daily prices. The three models are the mean-reverting jump-diffusion (MRJD) model with independent jump component, a Markov regime-switching (MRS) two-regime

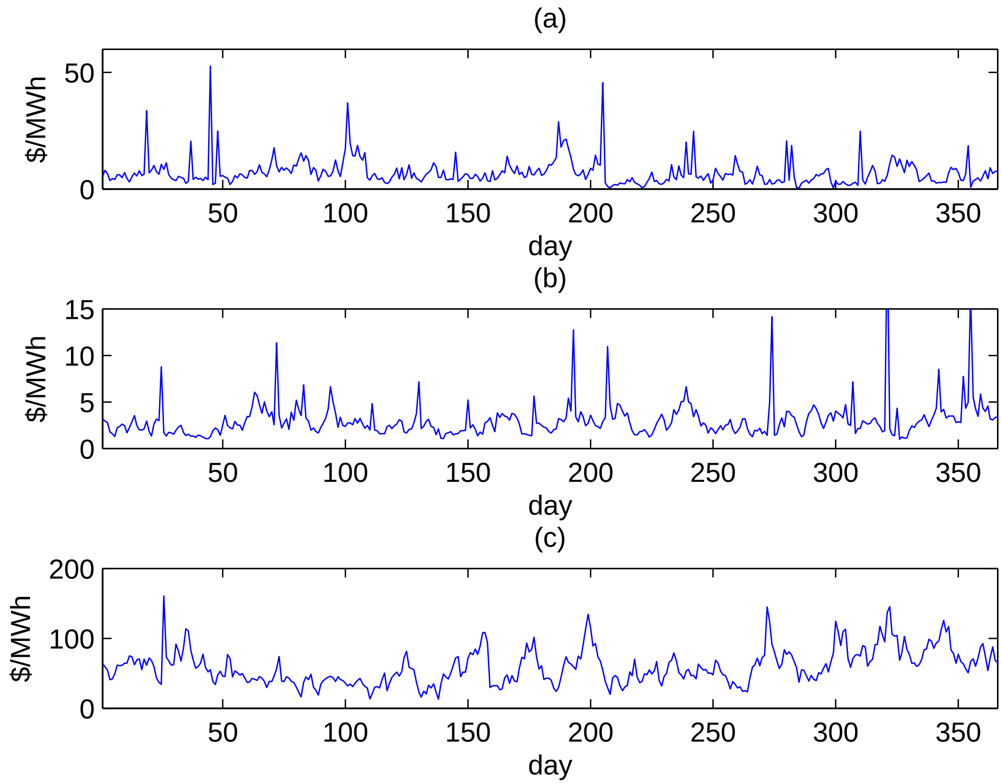

Figure 4.1: Sample price plots of the studied prices. (a) Ontario R10s, (b) New York R10n, (c) Ontario DOEP.

base-spike (BS) model with shifted spike, and a MRS three-regime base-spike-drop (BSD) model with shifted spike and shifted drop.

4.3.1 MRJD model

The first model is the MRJD model with independent jump/spike component. In this MRJD model, the spikes are modelled by an independent jump component so they do not distract the mean-reverting rate of the normal price process. As analyzed in Chapter 3, the reserve and regulation prices feature frequent and extreme jumps. Therefore, the MRJD model with an independent jump component is selected as a candidate model. The mathematical equation of this model is presented in (2.14) in Chapter 2. The jump occurrence is modelled by a Poisson process and the jump size is modelled by a Log-Normal distribution.

4.3.2 MRS two-regime base-spike model

The second selected model is the MRS two-regime BS model with shifted Log-Normal distribution for the spike regime. The MRS two-regime BS model captures spikes with a separate and independent spike regime. The base-regime is used to model the more moderate and smooth price process, i.e., the normal state of the price. The two regimes are independent of each other, and price can transit between the regimes with a certain probability. With this model, spikes can stay in the spike regime in the next time interval with a probability. This allows consecutive spikes or high price, which have been observed from price plots in Figure 4.1. In addition, the shifted Log-Normal distribution for the spike regime ensures that the spike regime does not capture low prices. Therefore, the MRS two-regime BS model with shifted spike regime is selected as another candidate model. The mathematical expression of this model is presented in (2.26) in Chapter 2.

4.3.3 MRS three-regime base-spike-drop model

It has been observed that when logarithmic transformation is performed on low prices, drops or negative spikes may be generated. The Cumulative density function (CDF) of the log de-seasonalized daily ONR10s is shown in Figure 4.2 as an example. This figure shows that the price has an obvious left tail which indicates there are drops in the price process. The three-regime base-spike-drop (BSD) model introduced in Chapter 2 separates drops from base regime, and thus could yield better modelling accuracy. In addition, the shifted Log-Normal distributions for the spike and drop regimes ensure that the spike regime only captures high prices and the drop regime only captures low prices. Therefore, the other selected candidate model is the three-regime base-spike-drop (BSD) MRS model with shifted

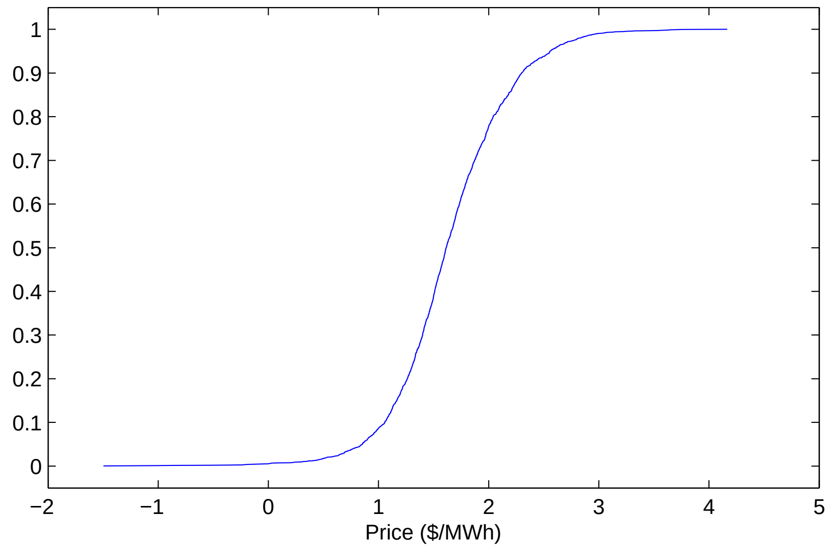

Figure 4.2: CDF curve of log de-seasonalized daily ONR10s

spike and drop regimes. The mathematical expression of this model is presented in (2.27) in Chapter 2.

4.4 Model calibration and performance measure

In this section, the employed model calibration procedures are demonstrated. The measures to evaluate performance of various models are also presented.

4.4.1 Model calibration

In the model calibration step, the parameters of the stochastic models are estimated using the observations, i.e., the historical data of the studied prices. Since the models are used to describe the stochastic components of the prices, deterministic components are firstly identified and removed.

As reviewed in Chapter 2, deterministic component of a price in the electricity market usually include a long term linear trend and seasonal components. The linear trend captures the long term price evolution in the market, and is detected by fitting a first order polynomial function to the prices. As presented in Chapter 3, there are daily, weekly, and annual seasonality in the prices in electricity market. The daily prices do not have daily seasonality which is intra-day pattern, so only weekly and annual seasonal components are to identified in these prices. The weekly seasonal component is determined using a moving average technique, while the annual seasonal component is represented by a sinusoidal function with a period of 365 days. The methodologies of calculating weekly and annual seasonal components are given in Chapter 2.

The stochastic models are then applied to the stochastic component. Model parameters are estimated with maximum-likelihood estimation (MLE). This estimation methodology, introduced in Chapter 2, finds the set of parameters that maximizes the likelihood function. The likelihood function reflects the overall probability density that every observation is generated by the model which is defined by a set of estimated parameters.

4.4.2 Goodness of fit

Measures based on log-likelihood function are widely used to evaluate goodness of fit of models for energy prices (e.g. [37,38,40,41,75]). In this thesis, the log-likelihood functions from model calibration are also used as an indicator of goodness of fit.

In addition to likelihood function, another popular way is to conduct an in-sample simulation which generates price trajectories using the calibrated models [33,40,41]. With the given first observation, the simulation generates the next observation using Monte-Carlo method, i.e., the price of next day, using the models with the estimated parameters. The simulation is terminated when the length of the trajectory reaches the length of the original price. For example, for an Ontario price which contains 2071 observations, the simulation uses the price of the first day as a starting value, and generates prices of the rest 2070 days.

In this thesis, 1000 price trajectories are simulated for each model and each price.

Several statistical measures are selected to evaluate how the price trajectories capture the distribution of the corresponding original price. Moments and percentile based measures specifically focus on distribution and dispersion captured by the model [33,41]. In the present work, the mean and standard deviation of the prices are selected as moment-based measures for the comparison. The higher order of moments, such as skewness and kurtosis, are not calculated as they are sensitive to few large spikes, but the main focus of this work is to compare the overall distributions. With this main focus in mind, in addition to the two moment-based measures, two other distributional measures, the interquartile range (IQR) and the interdecile range (IDR), are used to compare the performance of the models. These two quantile-based measures have been used in other similar studies [41]. IQR is defined as the difference between the third and first quartiles, which are 75% and 25% percentiles, respectively. IDR is defined as the difference between the 9th decile and first decile, which are 90% and 10% percentiles, respectively. IQR and IDR represent the dispersion of the studied prices.These four measures above are applied to the actual price and simulated price trajectories. Deviations of each measure are calculated between the actual prices and each of the 1,000 price trajectories. The average deviations are reported for each model.

4.5 Model calibration results

As discussed in Section 4.4, before model calibration the deterministic components are first removed from the prices, including linear trends and annual and weekly seasonality. Logarithmic transformation is then applied and log prices of the stochastic components are generated. The models are calibrated to fit the log prices of the stochastic components. All the simulation results in this chapter are based on log prices. Thus the units are not included in the discussions in the rest of this chapter.

Table 4.2: Estimated parameters of the MRJD model with Log-Normal jumps

Ontario	DOEP	ONR10s	ONR10n	ONR30
β	0.2012	0.3248	0.2631	0.2761
μ	4.0336	1.6345	1.2661	1.1407
σ	0.1772	0.3832	0.4306	0.4393
μ_j	1.5956	1.0866	0.9166	0.8812
σ_j	0.0673	0.2080	0.2999	0.2990
λ	0.0048	0.0087	0.0121	0.0101
Log L	643.9	-960.4	-1204.6	-1243.5
New York	LBMP6	NYR10s	NYR10n	NYReg
β	0.0585	0.2189	0.1671	0.1211
μ	4.2587	1.8041	0.9322	3.7126
σ	0.0902	0.3386	0.2325	0.1414
μ_j	1.5576	1.1087	0.6452	1.4475
σ_j	0.0325	0.1699	0.2271	0.0573
λ	0.0049	0.0063	0.0126	0.0119
Log L	1414.5	-482.0	61.2	764.9

4.5.1 MRJD model with independent jump component

For the MRJD model with independent jump/spike component, the first step of the calibration is to apply the jump filtering algorithm, reported in Chapter 2 to separate the jump component from normal prices. The mean-reverting process parameters are then estimated to fit the normal price process, and the jump sizes are fit to the Log-Normal distribution. The parameters and the log-likelihood functions of this MRJD model are presented in Table 4.2.

Parameters β, μ and σ belong to the mean-reverting process in (2.14). λ is the probability of the occurrence of jumps. μ_j and σ_j are the parameters of the Log-Normal distribution for the jump size. Log L is the value of log-likelihood function. A higher log-likelihood function indicates the model better fits the stochastic component of the price series. Note that the energy prices generally have much higher log-likelihood function than reserve prices, which implies the reserve prices are more difficult to model.

From these results, the fundamental characteristics of the reserve and regulation prices are captured by the estimated MRJD model. For instance, the positive mean-reversion rates β in Table 4.2 indicate that the mean-reversion property of the prices has been captured by the model. Price with mean-reversion property tends to go back to their long-term mean when it is off that level. The sample prices plotted in Figure 4.1 clearly show this property of the studied prices. Moreover, the non-zero λ values show that the model has also detected jumps in the prices. As presented in Section 2.4.1, the mean of the jump component can be calculated as $\exp(\mu_j + \sigma_j^2/2)$, which gives 4.9424, 3.0291, 2.6158, and 2.5242 for DOEP, ONR10s, ONR10n and ONR30, respectively. In the New York market, the mean of the jump components are 4.7501, 2.8098, 1.9562, and 4.2594, for LBMP6, NYR10s, NYR10n, NYReg, respectively. The mean of the jump component is higher than μ, the mean of the mean-reverting component, for all prices, which is as expected.

The primary differences between the characteristics of energy and reserve/regulation prices are also captured by the estimated MRJD models. Firstly, the mean values estimated for reserve prices are obviously lower than the energy prices. This is consistent with actual energy and reserve/regulation prices. Secondly, in Section 4.2.2, higher variability have been observed in reserve and regulation prices. The calibration results in Table 4.2 also show that the daily reserve and regulation prices, although smoother than hourly prices, still exhibit features of higher variability than energy prices, quantified by volatility parameter σ. In addition, the calibration results indicate that the spikes in reserve prices are more extreme compared to the energy prices, as revealed by the values of μ_j versus μ. This observation is consistent with the discussion in Section 4.2.2. The standard deviation parameter σ_j also appears to be higher than that of the energy prices, which indicates the spikes of reserve prices fluctuate more strongly than spikes in energy prices.

Table 4.3: Estimated parameters of the MRS two-regime BS model with shifted Log-Normal spike regime

Ontario	DOEP	ONR10s	ONR10n	ONR30
β_b	0.2262	0.3744	0.2850	0.1911
μ_b	4.0053	1.5466	1.1824	1.0443
σ_b	0.1654	0.3612	0.4010	0.4046
μ_s	-0.4800	-0.3885	0.0581	0.0298
σ_s	0.3675	0.5233	0.3465	0.3756
TS	4.0119	1.6134	1.2578	1.1198
$Prob_s$	0.0625	0.1464	0.1072	0.1168
Log L	782.7	-768.0	-959.6	-985.0
New York	LBMP6	NYR10s	NYR10n	NYReg
β_b	0.0561	0.2763	0.1771	0.1200
μ_b	4.2540	1.7008	0..8723	3.6723
σ_b	0.0875	0.3115	0.2088	0.1320
μ_s	-0.6272	-0.0896	-0.3165	-0.9286
σ_s	0.3681	0.4178	0.3755	0.3808
TS	4.2233	1.7237	0.9166	3.7322
$Prob_s$	0.0116	0.1302	0.1034	0.1241
Log L	1443.6	-363.9	194.3	870.4

4.5.2 MRS two-regime BS model

The MRS models are estimated using the Expectation-Maximization (EM) method which has been presented in Chapter 2. For this class of models, the detection of spikes is integrated in the parameter estimation of the regimes. The MRS models studied in this thesis deploy a mean-reverting process for the base regime, which represents the normal state of prices. The parameters and log-likelihood functions of the MRS two-regime BS model with shifted spike regime are displayed in Table 4.3.

In Table 4.3, subscript b designates base regime, and subscript s designates spike regime. β_b, μ_b and σ_b are the parameters of the mean-reverting process that models the base regime. μ_b and σ_b are parameters of the Log-Normal distribution that models the spike regime. $Prob_s$ is the unconditional probability that the price resides in the spike regime, i.e., the steady state probability of the Markov chain for the spike regime.

The mean-reversion property of all the studied prices are presented by the positive values of the mean-reversion rate parameter β_b. For the spike regimes, as introduced in Section 2.4.2.1, the mean implied by the model are calculated by $TS + \exp(\mu_s + \sigma_s^2/2)$. Therefore, the implied mean of the spike regime are 4.7202, 2.5050, 2.4528, and 2.3016 fore DOEP, ONR10s, ONR10n, and ONR30, receptively. And the implied mean of spike regime are 4.8349, 2.8123, 1.7557, and 4.1890 for LBMP6, NYR10s, NYR10n, and NYReg, respectively. The mean of the spike regime are all higher than the mean of the base regime, μ_b, as expected. The parameters in Table 4.3 show that this model also captures the main characteristics of the studied prices, including the mean-reversion property and spikes.

The results presented in Table 4.3 also show that the MRS models captures the basic differences among of the studied prices. The energy prices have higher mean in both base and spike regimes, which are generally above 4 while the mean of reserve prices are generally below 3. On the other hand, the reserve and regulation prices generally have higher volatility σ than energy prices in both regimes. For example, the base regime volatility σ_b of Ontario reserve prices are all above 0.3, whereas σ_b is 0.1654 for DOEP. The steady state probabilities of the spike regime, $Prob_s$, are also generally much higher in reserve and regulation prices, which indicate that spikes are more frequent in these prices when compared to the energy prices.

Although both the MRJD model and the MRS BS model capture the main characteristics of the prices, the two models perform differently in the identification of the excited state, which is the jump state or spike regime. The occurrence probability of spikes is higher in the MRS model compared to λ in the MRJD model which is the probability of jumps. The main reason is that the MRJD model filters jumps only, whereas the spike regime of the MRS model captures all prices that are significantly higher than the normal state. The MRJD model filters the jumps by price changes rather than prices themselves. For example, if the price jumps significantly to a high level and stays the same for a few days, the price change will only become large in the day when the jump occurs, and it will stay at 0 in the days that the price does not change. Therefore, only the price after the jump will be captured by the jump component in the MRJD model, and the subsequent high prices will be identified to be in normal state. The MRS model, on the other hand, tends to identify all these high prices to be in spike regime. Moreover, the two models identify the excited states, i.e. jumps or spike, in different ways. In the MRJD model the jumps are detected by a pre-specified threshold. However, in MRS model the spikes status is represented by a Markov Chain and determined by overall likelihood. In other words, the MRJD model has a fixed threshold for classifying normal prices and jumps. However, the MRS model applies optimization to determine if a price is in spike regime.

From Table 4.2 and 4.3, one can observe that the log-likelihood functions of the MRS model tends to be slightly higher than the ones of MRJD model for most prices. This indicates that the MRS model generally outperforms MRJD model for the studied prices. Further comparison of goodness of fit is presented in Section 4.6. Reserve and regulation prices generally see a more substantial increase in their log-likelihood functions when switching from MRJD model to MRS model. This observation implies that the MRS model outperforms the MRJD model more when applied to reserve and regulation prices, and thus is a more appropriate model for these prices.

4.5.3 MRS three-regime BSD model

The MRS three-regime BSD model with shifted Log-Normal spike and drop regimes is calibrated for the studied prices and the estimation results are shown in Table 4.4. The parameters of the base, spike, and drop regimes represent the main characteristics in each regime. Similar to the MRS BS model in Section 4.5.2, the MRS BSD model aslo captures the main characteristics in the prices such as mean-reverting property and existence of spikes. The differences between the energy prices and the reserve and regulation prices are

Table 4.4: Estimated parameters of the MRS three-regime BSD model with shifted Log-Normal spike and drop regimes

Ontario	DOEP	ONR10s	ONR10n	ONR30
β_b	0.3057	0.4192	0.3683	0.3537
μ_b	4.0021	1.5596	1.2467	1.1022
σ_b	0.1502	0.3078	0.3158	0.3263
μ_s	-0.6291	-0.3911	-0.0254	-0.0485
σ_s	0.4020	0.5021	0.3685	0.3969
μ_d	-0.6985	0.0193	-0.3256	-0.3521
σ_d	0.4078	0.4251	0.6211	0.6155
TS	4.0119	1.6134	1.2578	1.1198
TD	4.0119	1.6134	1.2578	1.1198
$Prob_s$	0.1068	0.1734	0.1529	0.1609
$Prob_d$	0.0509	0.0379	0.1421	0.1383
Log L	926.6	-450.8	-593.3	-641.5
New York	LBMP6	NYR10s	NYR10n	NYReg
β_b	0.0564	0.3299	0.3117	0.3400
μ_b	4.2668	1.6720	0.9009	3.7101
σ_b	0.0852	0.2566	0.1799	0.1023
μ_s	-0.6191	-0.2341	-0.5588	-1.1554
σ_s	0.3620	0.4473	0.4450	0.4862
μ_d	-0.7093	-0.3932	-0.5214	-0.6730
σ_d	0.1845	0.4424	0.2926	0.3107
TS	4.2233	1.7237	0.9166	3.7322
TD	4.2233	1.7237	0.9166	3.7322
$Prob_s$	0.0117	0.2131	0.1948	0.2271
$Prob_d$	0.0337	0.0629	0.1276	0.1750
Log L	1418.9	-131.0	386.7	1034.0

also captured. The analyses are similar to those in Section 4.5.2 so they are not repeated here.

In the BSD model, the differences among the three regimes are also correctly captured. Since the spike and drop regimes are modelled by Log-Normal distribution, as introduced in Section 2.4.2.2, the implied mean is $TS + \exp(\mu + \sigma^2/2)$ for the spike regime, and $TD - exp(\mu + \sigma^2/2)$ for the drop regime. For all the studied prices the mean of the spike regimes are higher than the base regimes, and the mean of the drop regimes are lower than the base regimes. Moreover, from Table 4.4 it can be observed that the base regimes have the lowest volatility parameters σ among the three regimes. It is reasonable that the spike and drop regimes have higher volaitility because they capture the most extreme high and low prices, which contain positive and negative jumps.

The log-likelihood functions in Table 4.4 are higher than those in Table 4.2 and 4.3 in most of the studied prices. The only exception is the energy price in the New York market, for which the log-likelihood function of the BSD model is slightly lower than that of the BS model. The generally higher log-likelihood functions indicate that the three-regime BSD model yield the best overall fit among the three models.

Although similar in structure, the parameters of the three-regime BSD model show differences compared to the two-regime BS model. In the BSD model, the volatility parameter of the base regime σ_b are generally lower in all the studied prices. In the BS model only the spikes are taken away from base regime. However, in the BSD model the low price drops have also been taken away from the base regime, and thus only the most moderate prices are captured by the base regime, which are less volatile and dispersive. However, the mean of the base regime, $mean_b$, are not always higher than those in the BS model, because the spike identification has also been affected by the structure change of the model.

4.5.4 Difference from existing work

As reviewed in Chapter 1, the reserve price in the German market has been modelled in [30]. There are two major differences between the work in this chapter and the work [30]. First, the regime-switching models applied in the present chapter have the flexibility to assign any specifications to the regimes that describe the stochastic component of the price. However, in [30] the regime-switching scheme is used to model the error term of the ARMA model, and both regimes are represented by a Gaussian distribution. Second, the present chapter studies reserve and regulation prices in North American markets, whereas

[30] studies reserve price in the German market. These reserve prices represent different characteristics due to different market design, which have been discussed in Chapter 3. For example, the German reserve prices have lower volatility than energy prices, whereas in the studied North American markets, the reserve prices present significantly higher volatility than energy prices.

4.6 Performance comparison between models

The quantities of the selected measures in Section 4.4 and their corresponding deviations are presented in Table 4.5, 4.6, 4.7. In these tables, Act, Sim, and Dev denotes actual, simulated, and deviation respectively. The deviations are positive when the statistical measures of the simulated prices are higher than those of the actual prices. For example, for ONR10n, the simulated mean is higher than the actual mean by 0.7% with the MRJD model.

Table 4.5: Moment and quantile based measures of prices in Ontario and New York

		MRJD					
		ONR10s	ONR10n	ONR30	NYR10s	NYR10n	NYReg
Mean	Act	1.65	1.29	1.16	1.81	0.94	3.72
	Sim	1.66	1.30	1.17	1.82	0.95	3.76
	Dev	0.7%	0.7%	0.6%	0.6%	1.4%	1.2%
STD	Act	0.53	0.65	0.65	0.55	0.43	0.30
	Sim	0.59	0.70	0.69	0.59	0.47	0.54
	Dev	11.1%	7.5%	5.5%	6.8%	9.4%	80.4%
IQR	Act	0.63	0.75	0.76	0.69	0.66	0.31
	Sim	0.71	0.87	0.87	0.73	0.57	0.40
	Dev	12.1%	16.1%	13.5%	6.4%	16.4%	29.5%
IDR	Act	1.24	1.59	1.64	1.36	1.10	0.82
	Sim	1.35	1.67	1.66	1.41	1.10	0.77
	Dev	8.9%	4.4%	0.8%	3.2%	-0.3%	-6.4%

The results in Table 4.5, 4.6, 4.7 show that while the MRJD model has a decent fit, the two MRS models have better captured the mean, standard deviation, IQR and IDR in most

Table 4.6: Moment and quantile based measures of prices in Ontario and New York with the two-regime base-spike (BS) model

		MRS					
		ONR10s	ONR10n	ONR30	NYR10s	NYR10n	NYReg
Mean	Act	1.65	1.29	1.16	1.81	0.94	3.72
	Sim	1.67	1.31	1.18	1.83	0.95	3.73
	Dev	1.3%	1.7%	2.1%	1.2%	1.4%	0.3%
STD	Act	0.53	0.65	0.65	0.55	0.43	0.30
	Sim	0.54	0.67	0.67	0.56	0.44	0.31
	Dev	2.4%	2.6%	2.7%	2.3%	1.5%	2.5%
IQR	Act	0.63	0.75	0.76	0.69	0.66	0.31
	Sim	0.73	0.90	0.90	0.73	0.57	0.44
	Dev	15.6%	20.1%	17.8%	5.3%	16.2%	40.4%
IDR	Act	1.24	1.59	1.64	1.36	1.10	0.82
	Sim	1.35	1.72	1.70	1.40	1.11	0.79
	Dev	8.8%	7.8%	3.7%	2.5%	0.9%	-3.7%

Table 4.7: Moment and quantile based measures of prices in Ontario and New York with the three-regime base-spike-drop (BSD) model

		MRS					
		ONR10s	ONR10n	ONR30	NYR10s	NYR10n	NYReg
Mean	Act	1.65	1.29	1.16	1.81	0.94	3.72
	Sim	1.66	1.28	1.16	1.82	0.94	3.71
	Dev	0.9%	0.4%	0.1%	0.7%	1.1%	-0.3%
STD	Act	0.53	0.65	0.65	0.55	0.43	0.30
	Sim	0.55	0.68	0.69	0.56	0.43	0.31
	Dev	2.51%	4.7%	5.3%	2.8%	0.3%	2.9%
IQR	Act	0.63	0.75	0.76	0.69	0.66	0.31
	Sim	0.67	0.81	0.84	0.71	0.55	0.37
	Dev	5.7%	7.6%	10.6%	2.7%	12.1%	18.3%
IDR	Act	1.24	1.59	1.64	1.36	1.10	0.82
	Sim	1.28	1.61	1.63	1.38	1.10	0.77
	Dev	2.9%	1.1%	0.8%	1.0%	0.6%	-6.5%

prices. Note that the two MRS models generally have lower errors than the MRJD model, which indicate better goodness of fit. The mean and standard deviation describe the main price level and fluctuation, while the IQR and IDR describe the dispersion range showing how the price time series span. Thus, the generally lower deviations in Table 4.6 and 4.7 show that the MRS models well capture both price level and dispersion and hence, the main distribution of the studied reserve and regulation prices. Moreover, the log-likelihood funtions with the MRS BS and BSD models in Table 4.3 and 4.4 are also generally higher than those of the MRJD model in Table 4.2. To sum up, the MRS class of models appear to be more appropriate models for the studied reserve and regulation prices.

The moment based measures have been used in [33] for daily energy prices and the deviations were 0% - 1% for mean and 0% - 11% for standard deviation. IQR and IDR measures have been used in [41], where the deviations of IQR and IDR were within 26% and 22% respectively with a similar two-regime model, and were within 8% and 5% respectively for a similar three-regime model. Although a direct comparison is not possible because these two researches focused on energy price modelling in different markets, the deviations of the MRS models in Table 4.6 and 4.7 are reasonable compared to the existing literature.

Between the two MRS models, the three-regime BSD model presents a better overall fit demonstrated by the generally smaller deviations compared to the two-regime BS model. Most of the deviations in mean, IQR and IDR are smaller with the three-regime BSD model.The deviations in standard deviation are a bit less satisfying with the BSD model but are close the the two-regime BS model.

The better fit of the BSD model originates from the characteristics of the reserve and regulation prices. Due to the low price levels in these price, the logarithmic transformation has created drops. In the BS model, the spike regime does not capture any price under TS which is median. As a result, the drops are captured by the base regime and thus the parameters of the base regime will be distorted. On the other hand, the BSD model has a drop regime to model these drops and thus the base regime won't be affected. This can be further demonstrated by the calibrated parameters shown in Table 4.3 and 4.4. The base regime of the BS model tend to have greater volatility paramter σ_s than those in the BSD model.

The CDF plot shown in Fig 4.2 further explains the above point. It can be observed that the log price have a clear left tail which is caused by the drops. The left tail in the reserve price is clearly longer than in the energy price, which indicates the drops are more extreme in the reserve price.

Among the studied prices, it can be observed that, as expected, the prices with higher variability are generally more difficult to model, demonstrated by greater deviations in the statistical measures.

4.7 Conclusion

Reserve and regulation prices are characterized by higher volatility, lower mean, more frequent price spikes and a more skewed distribution compared to electric energy prices, thus modelling their behavior is potentially more challenging. In this chapter, an attempt was made to model the prices of operating reserve and regulation services in Ontario and New York competitive electricity markets. Three models, i.e., a MRJD model with independent jump component, a MRS two-regime BS model, and a MRS three-regime BSD model, were applied to the daily average of reserve and regulation prices, and their performance in capturing the main characteristics of actual price time series was compared. In particular, the mean, standard deviation, IQR and IDR of the simulated and actual prices were compared.

The presented simulation results show that while all the three models reasonably captured the main features of the studied prices, the three-regime BSD MRS model better fits the reserve and regulation prices. The better performance of the three-regime MRS model is a result of the multi-regime nature in these prices. Prices in electricity markets are affected by various factors such as the availability of generation resources, congestion of transmission lines, demand fluctuation, and changes in other operating conditions in the system. These factors will result in variations in the price patterns for both energy and reserve prices. Furthermore, the existence of low prices caused price drops, especially after the logarithmic transformation. Therefore, the MRS three-regime BSD model, which captures the changes of price patterns by a Markov process with base, spike and drop regimes, is able to provide a better representation of the dynamics in the reserve and regulation prices. The MRS three-regime BSD model can be applied in the financial market for risk control and pricing regarding the operating reserve and regulation services.

Chapter 5

Modelling Hourly Reserve Prices with Three-Regime MRS Models

5.1 Introduction

Hourly reserve and regulation prices exhibit different characteristics and patterns compared to daily prices due to intra-day fluctuations. Spot market operations in the three studied electricity markets are based on hourly settlement. Therefore, a thorough understanding of the hourly price dynamics and distributions provides valuable information for risk management and derivative pricing in the spot market. This chapter investigates the application of several stochastic models for hourly reserve prices to study the price dynamics and distribution.

In this chapter, the studied reserve price is decomposed into deterministic and stochastic components in Section 5.2. In Section 5.3, a two-regime base-spike (BS) model and a three-regime base-spike-drop (BSD) model are applied to the logarithm transformed (log) reserve price, and the performance of these models is compared. In Section 5.4, the modelling of original hourly reserve price is investigated. The two-regime BS model and three-regime BSD model used in Section 5.3 are applied to the original hourly reserve price, and a new three-regime base-spike-extreme (BSE) model is proposed. The performance of these three models is analyzed and compared in this section. Moreover, a comparison to the log-price models is also provided in this section. The modelling results are then concluded in Section 5.5.

5.2 Modelling hourly price

As discussed in Chapter 3, reserve and regulation prices generally present similar characteristics such as low price levels, higher variability, and frequent and extreme jumps or spikes. For the convenience of presenting and comparing the performance of various models for the hourly prices, in this chapter, price modelling is analyzed in detail for one typical reserve price.

The 10-minute spinning reserve in the Ontario market, denoted as ONR10s, is selected to be the sample price to be studied in detail in this chapter. Since the other reserve and regulation prices follow similar characteristics, the modelling results for ONR10s can be extended to these prices. To better present the characteristics of the studied price and the performance of the models, the hourly price is studied in a time frame of 3 months. For ONR10s, the period of August 1, 2004 to October 31, 2004 is selected, which covers 91 days or 2184 hours.

Price plot of ONR10s in the studied period is shown in Fig 5.1(a). As discussed in Chapter 4, the hourly prices generally feature larger dispersion than daily ONR10s.

The decomposition of deterministic and stochastic components is presented in the rest of this section. The distinguishing characteristics of the hourly reserve price is then demonstrated which provides a basis to building models for this price.

5.2.1 Modelling the deterministic component

As discussed in Chapter 2, the price time series needs to be first decomposed to deterministic and stochastic components. The deterministic component consists of a long-term linear trend and seasonality components. And as discussed in Chapter 3, hourly reserve and regulation prices exhibit daily, weekly and annual seasonality.

Different from the deseasonlization of daily prices in Chapter 4, daily seasonality needs

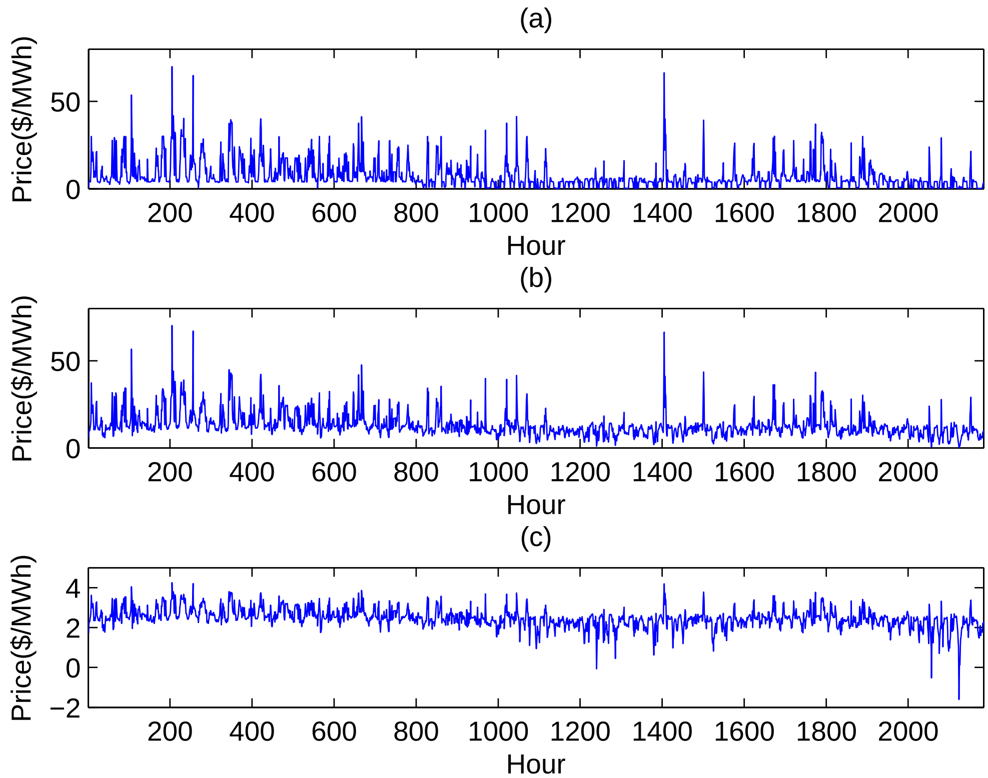

Figure 5.1: Sample price plots of ONR10s. (a) Hourly ONR10s, (b) Shifted de-seasonalized ONR10s, (c) Log de-seasonalized ONR10s.

to be accounted for when modelling hourly prices. Moreover, the annual seasonality is not presented in the studied hourly price data, because the length of the studied period is less than one year. Therefore, the seasonality component of the studied hourly price only consists of daily and weekly cycles. As introduced in Chapter 2, the daily and weekly seasonality components are both identified by the moving average technique. Following the same fashion as in Chapter 4, the de-seasonalized prices are shifted so that it has the same minimum as the prices before deseasonalization.

A price plot of the de-seasonalized ONR10s is presented in Fig 5.1(b). The log de-seasonalized prices are plotted below in Fig 5.1(c). For convenience in presentation, the deseasonalization is not repeated in the rest of this chapter when referring to the de-seasonalized prices. For example, the log-transformed de-seasonalized price will be called log prices.

5.2.2 Modelling the stochastic component

It can be observed in Figure 5.1(c) that there are significant drops, called negative spikes, in the log hourly ONR10s. The existence of drops in log daily prices have been discussed in Chapter 4. However, in the log hourly reserve prices, the drops are more significant and frequent. The CDF of the studied log hourly ONR10s price is displayed in Figure 5.2. Compared to the CDF of the log daily ONR10s in Figure4.2, the CDF of the log hourly ONR10s has a longer left tail, indicating more extreme drops. As discussed in Chapter 4, hourly prices have higher dispersion than the daily prices. In other words, both very low prices and very high prices exist in hourly reserve prices. The very low prices will result in large negative values when applying the logarithmic transformation. These low prices are smoothened by daily averaging, thus the drops are less significant in the log daily prices.

With the significant drops and higher dispersion, the hourly reserve and regulation prices require modelling techniques specifically designed for them. In the rest of this chapter, several models are proposed and applied to the studied reserve price ONR10s and their performance are studied.

In addition, most of the existing research model log energy prices. The logarithmic transformation was taken for these prices in order to mitigate the positive jumps or spikes with the ultimate objective of better modelling these prices. However, as discussed above, log hourly reserve prices have a large number of extreme drops, which introduce challenges to price modelling. Therefore, in addition to modelling the log price, in this chapter the models are also built for the original prices before logarithmic transformation is applied.

5.3 Modelling log hourly reserve prices

It can be observed that the CDF of the log hourly ONR10s in Figure 5.2 has two obvious tails, one spreading left and one spreading right. The left and right tails imply the existence of drops and positive spikes in the log price, respectively. As discussed in Section 5.2, the left tail is caused by the very low prices in the original price time series. However, at the same time, there also exist extremely high prices in the original price time series, which form positive spikes after logarithmic transformation. The existence of these high prices and the resulted postive spikes can be observed in Fig 5.1(b) and (c). The left tail in the CDF is longer than the right tail, which indicates the negative spikes are more extreme than the positive spikes in log hourly reserve prices. With the existence of both left and right tails, the two-regime base-spike (BS) model used in Chapter 4 is not enough to model such price time series. The three-regime base-spike-drop (BSD) model should be a more appropriate model for the log hourly reserve prices and are applied in this section. The two-regime base-regime (BS) model is also applied for comparison purposes.

5.3.1 Three-regime base-spike-drop model with shifted spikes and shifted drops

The MRS three-regime BSD mode has been applied in Chapter 4 to capture the drops and spikes in the log daily price processes. This model uses shifted Log-Normal distributions to represent the spike and drop regimes. The equations of this model are presented in (2.27) in Chapter 2. The MRS two-regime BS model applied in this section for comparison has been presented in (2.26) in Chapter 2.

5.3.2 Model calibration

The BSD model is applied to the log hourly price of ONR10s. The TS and TD values are set as medians of the log de-seasonalized ONR10s so $TS = TD = 2.3618$. In Table 5.2, $Prob_S$ and $Prob_D$ are the unconditional probabilities of the price residing in the spike

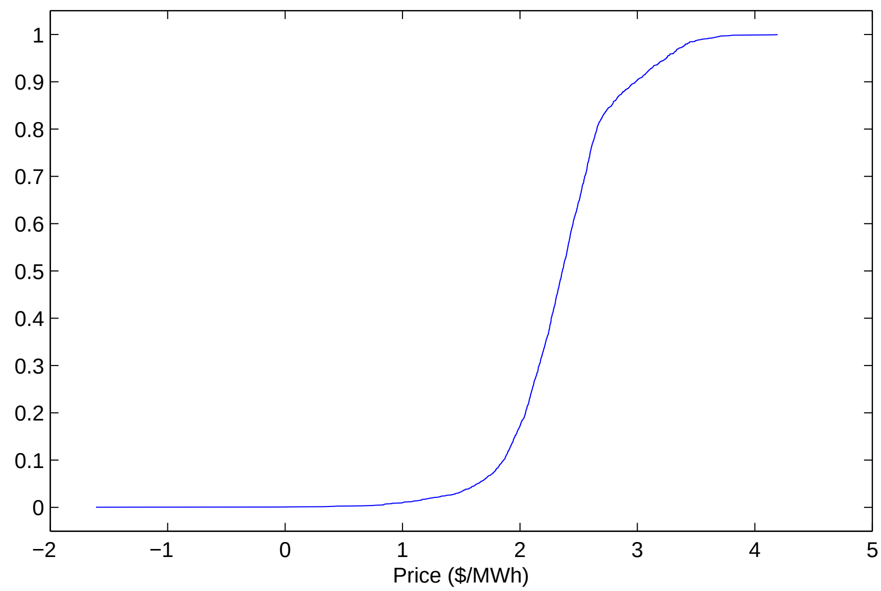

Figure 5.2: CDF curve of log de-seasonalized ONR10s

regime and drop regime, respectively. The two-regime base-spike (BS) model with shifted spike, which was used in Chapter 4 for the daily prices, are also applied to the log hourly ONR10s for comparison purpose. The two-regime BS model has a base regime modelled by a mean-reverting process, and a spike regime modelled by a shifted Log-Normal distribution with TS being the median, i.e., $TS = 2.3618$. The estimated parameters are shown in Table 5.2. The log-likelihood function is 335.4 for the BSD model, and -526.1 for the BS model.

The mean of the spike and drop regimes implied by the BSD model are calculated as presented in Section 2.4.2.2, using the estimated parameters of the Log-Normal distributions of the corresponding regime. The calculated model-implied mean is 3.0991 and 1.6819 for the spike and drop regimes, respectively. As expected, the mean of the base regime, which is 2.3494, is lower than the mean of the spike regime, and higher than the mean of the drop regime. Both spike and drop regimes have higher volatility σ than the

Table 5.1: Estimated parameters of the three-regime base-spike-drop (BSD) model and the two-regime base-spike (BS) model for log ONR10s

Model	Regime	β	μ	σ	TS/TD	$Prob_s$ / $Prob_d$
BSD	Base	0.2751	2.3494	0.1852	N/A	N/A
	Spike	N/A	-0.4106	0.4601	2.3618	0.1552
	Drop	N/A	-0.5521	0.5766	2.3618	0.1282
BS	Base	0.3194	2.3235	0.3198	N/A	N/A
	Spike	N/A	-0.0426	0.2595	2.3618	0.0462

base regime because the fluctuations become more significant outside the normal status. The unconditional probabilities show that the spike regime captures 15.52% of observations and the drop regime captures 12.82% observations, which take a large portion of the total observations. Therefore, the base regime only captures the moderate fluctuations, and thus, it's volatility is relatively small compared to the spike and drop regimes. The positive value of β indicates the log ONR10s still has a mean-reversion property.

On the other hand, the BS model's base regime needs to pick up the negative drops, which results in a much higher volatility parameter σ in the base regime compared to the BSD model. With this higher $sigma$, the base regime of the BS model also picks up many positive high values which, in the BSD model, are captured by the spike regime. As a result, with the BS model, the probability of residing in spike regime, which is 0.0462, is much lower than that of the BSD model. Only very high prices are captured by the spike regime with the BS model, thus causing a higher value of μ in the spike regime, and a lower value of σ in the spike regime.

The calibration results of transition probability matrix is shown in Table 5.2. The diagonal transition probabilities are all higher than 0.5, which imply that the probability of staying at the current regime is higher than the probability of jumping to another regime. Therefore, the existence of consecutive spikes is recognized by this model, which on the other hand indicates that the assumption made in [34, 37] that spikes only last one time

Table 5.2: Estimated Probability Transition Matrix of the three-regime model for log ONR10s

ONR10s	Base Regime	Spike Regime	Drop Regime
Base regime	0.9046	0.0543	0.0411
Spike regime	0.2290	0.7226	0.0485
Drop regime	0.2201	0.0461	0.7338

interval is not valid for the studied hourly reserve prices. Another observation is that the transition probabilities between the spike and drop regimes are non-zero too, although they are much smaller compared to other transition probabilities. On one side, the transition between the spike and drop regimes imply that the fluctuation in the hourly reserve price is significant. On the other side, the drops or negative spikes in the log reserve prices are generated by the logarithmic transformation. Therefore, a drop in the log price may not be a drop in the original price, so it is possible it can jump to the spike regime given the high variability of the reserve and regulation prices.

To present the accuracy of categorizing prices into regimes, the identifications of spikes and drops with the BSD model are displayed in Fig 5.3. For each hour, $Prob(S)$ is the probability that the price is identified as a spike, while $Prob(D)$ is the probability of being in the drop regime. It can be observed that, the $Prob(S)$ is high when there is a spike in the price in Fig 5.3(a), and $Prob(D)$ is high when there is a drop in the price. Therefore, the three-regime BSD model presents good accuracy on spike and drop identifications. On the other hand, with the two-regime BS model, the drops have to be captured by the base regime. As a result, the base regime of the two-regime model has a lower long term mean μ of 2.3235. In addition, the drops also bring the base regime volatility σ higher in the two-regime model to 0.3198, compared to 0.1852 in the base regime in the three-regime BSD model.

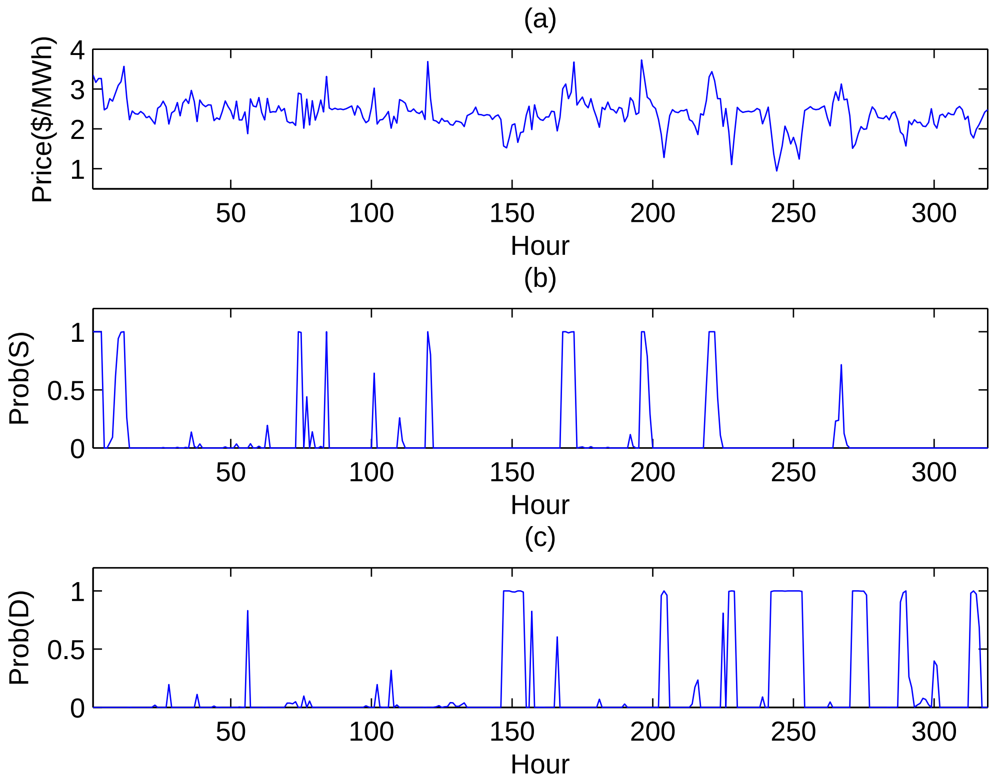

Figure 5.3: (a) Log de-seasonalized ONR10s (b) Probability of being in spike regime with three-regime base-spike-drop (BSD) model (c) Probability of being in drop regime with three-regime BSD model

5.3.3 Goodness-of-fit analysis

The log-likelihood function of the BSD model is 335.4, which is higher than the log-likelihood function of the BS model which is -521.6. The higher log-likelihood indicates a better overall fit with the BSD model. In addition to the log-likelihood function, other goodness-of-fit measures applied to daily price models in Chapter 4, being the moment and quantile based measures, are also applied here to compare the performance of the two models. The results are shown in the Table 5.3. It can be observed that the two-regime BS model matches the mean and STD very well, but causes deviations in distributional measures IQR and IDR. The three-regime BSD model has significantly improved the accuracy of distribution match, and also provides good match to the moments based measure.

However, although better than the two-regime BS model, the three-regime BSD model still has a large IQR deviation. The IQR of the simulated prices from the BSD model is 0.5480, which is 10.89% higher than the IQR of the actual price. The simulated prices from the BSD model presents a larger number of significant positive spikes than the actual price, but presents fewer moderate high prices, which increases the price span and causes a larger IQR than the actual price.

Table 5.3: Statistical measures of goodness-of-fit with the three-regime base-spike-drop (BSD) model and two-regime base-spike (BS) model for log ONR10s

		Mean	STD	IQR	IDR
Actual		2.3681	0.4817	0.4941	1.1263
BSD	Simulated	2.3687	0.5011	0.5480	1.1310
	Deviation	0.03%	4.02%	10.89%	0.42%
BS	Simulated	2.3738	0.4907	0.6316	1.2486
	Deviation	0.24%	1.86%	27.82%	10.86%

As discussed in this section, the logarithmic transformation has caused significant drops in the hourly reserve price. To avoid the extra challenges in modelling caused by these significant drops, the original price before logarithmic transformation is modelled in the next section.

5.4 Modelling original hourly reserve price

In most of the existing literature on modelling electric energy prices, stochastic models are built for log prices rather than the original prices. Log energy prices tend to be less volatile and less dispersive and thus easier to model. Logarithmic transformation has the characteristic that it compresses the difference between two numbers that are greater than

1, but amplifies the difference when the numbers are less than 1. Since energy prices are much greater than 1 in most time, the logarithmic transformation compresses fluctuations in these prices and thus improve the modelling accuracy.

However, as observed in Chapter 3, the reserve prices are generally much lower than the energy prices. The hourly reserve prices have a relatively large number of low prices that are below 1 $/MWh where logarithmic transformation will create negative spikes. And as a result, a separate drop regime was required to model the negative spikes, as analyzed in Section 5.3. Taking logarithmic transformation for hourly reserve prices doesn't help reduce volatility and dispersion as it does to daily energy prices. On one hand, the logarithmic transformation compresses fluctuations of positive spikes which benefits modelling. On the other hand, it also produces new negative spikes which makes modelling less accurate.

Although most existing literature developed models for log prices, there are a few publications that have focused on original prices [39,41]. The simulation results in these works have shown that modelling prices themselves can also provide satisfying goodness-of-fit. In this section, several established models and a new model are proposed for hourly reserve prices. The performance of these models are compared with each other, and are further compared with the models for the log prices used in Section 5.3.

5.4.1 Characteristics of the original reserve price

The de-seasonalized hourly reserve price ONR10s is ploted in Fig 5.1(b). The plots show there are fewer negative spikes in the original prices than in the log prices. In addition, the negative spikes in the original prices are generally more moderate than in log prices. However, the positive spikes in the original prices are more significant than the log prices.

The CDF of the de-seasonalized ONR10s is presented in Fig 5.4. Compared to CDF of the log prices in Fig 5.2, the CDF of the original prices presents a shorter left tail which indicate much less extreme drops. On the other hand, the right tail of the CDF is longer,

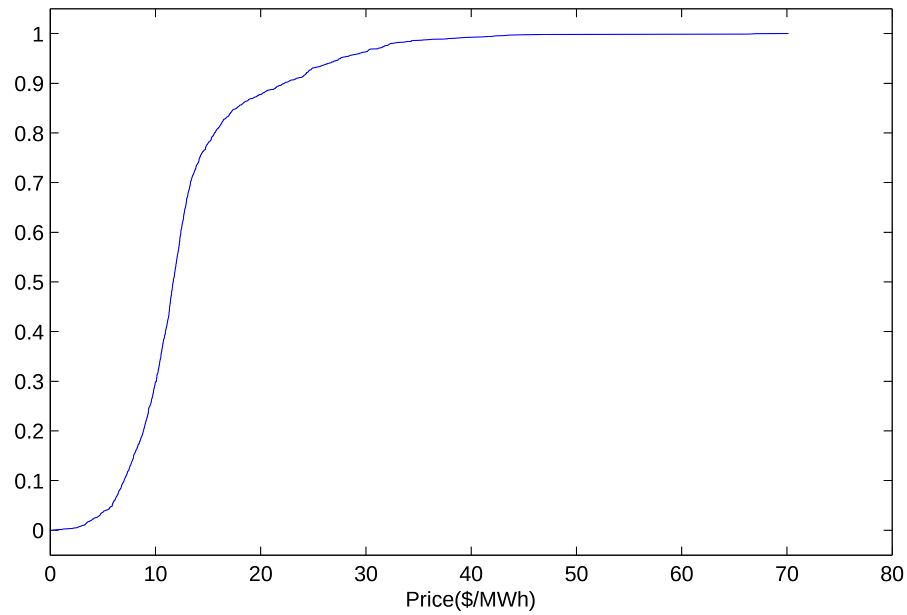

Figure 5.4: CDF curve of the de-seasonalized ONR10s

indicating that the original prices feature more severe positive spikes than the log prices.

Since the drops in the original prices are less significant than the log prices, a two-regime base-spike (BS) model is utilized. The three-regime base-spike-drop (BSD) model is another candidate to incorporate the modelling of drops. Although drops in the original prices are less significant, they do exist in the price process and form a left tail in the CDF.

As the original prices have frequent positive spikes, some of which are extreme, a new three-regime model is proposed that features one base regime and two spike regimes. One spike regime is used to model the moderate high prices, while the other spike regime only captures the most extreme jumps and spikes in the price process. This new proposed model is denoted as a three-regime base-spike-extreme (BSE) model.

The above three models are applied to the de-seasonalized original reserve price ONR10s and their performance are compared using log-likelihood function and other statistical measures that have been applied to previous models.

Table 5.4: Estimated parameters of the two-regime base-spike (BS) model for ONR10s

Regime	β	μ	σ	TS	$Prob_s$
Base	0.2811	9.8709	2.1328	N/A	N/A
Spike	N/A	2.2528	0.6717	10.6099	0.1791

5.4.2 Two-regime base-spike model

As observed from the CDF of the de-seasonalized ONR10s in Figure 5.4, there is a long right tail, which corresponds to the of extremely high prices and spikes in the price process. The left tail, on the other side, is much shorter than the right tail which correspond to drops, which are much more moderate than the positive spikes. Therefore, the drop regime may not be necessary and a two-regime BS model can be a good candidate given the simple structure. A model with fewer regimes and parameters has the benefit of lower computation burden and time.

The two-regime BS model is the same as the one used in Section 5.3 and the equations of this model are presented in (2.26) in Chapter 2. The threshold of the spike regime, TS, is set to median again. The parameters are estimated and shown in Table 5.4. The log-likelihood function is -5135.2.

The positive mean-reversion parameter β of the base regime indicates the two-regime BS model captures mean-reversion property in the price. For the spike regime, the mean implied by the model is calculated using the estimated μ and σ of the spike regime as $TS + \exp(\mu + \sigma^2/2)$, and the result is 22.5320. As expected, the mean of the spike regime is significantly higher than the mean of base regime which is 9.8709.

The transition matrix of the two-regime BS model is presented in Table 5.5. Both the diagonal probabilities are significantly non-zero, indicating that the prices tend to stay in the regime it currently resides in. It is also observed that the spike regime has a higher probability of transition to the base regime, which implies the expected duration of staying

Table 5.5: Estimated probability transition matrix of the two-regime (base-spike (BS) model for ONR10s

Regime	Base	Spike
Base regime	0.9406	0.0594
Spike regime	0.2722	0.7278

Table 5.6: Statistical measures of goodness-of-fit with the two-regime base-spike (BS) model for ONR10s

	Mean	STD	IQR	IDR
Act	11.98	6.43	5.24	13.40
Sim	12.12	6.77	5.54	12.99
Dev	1.2%	5.3%	5.6%	-3.1%

in spike regime is shorter than that of the base regime. This is consistent with observations in the price process, because the prices in the spike regime are usually caused by temporary events such as demand increase or outage of transmission lines or generation facilities. These high prices may last for a short period but will finally drop back to a long-term stable level based on the actual cost of providing reserve service.

The statistical measures are applied to the simulated prices and the results are displayed in Table 5.6. All four measures are well captured, with the largest deviation percentage being only 5.63%.

5.4.3 Three-regime base-spike-drop model

The existence of drops in the hourly reserve price ONR10s suggests that the three-regime base-spike-drop (BSD) model can still be a reasonable representation of the dynamics and distribution in this price. Therefore, in this section the three-regime BSD model is applied to the studied original hourly reserve price as another model candidate. The three-regime BSD model applied here is the same as the one applied to the log price in Section 5.3.1 and

Table 5.7: Estimated parameters of the three-regime base-spike-drop (BSD)model for ONR10s

Regime	β	μ	σ	TS/TD	$Prob_s$ / $Prob_d$
Base	0.2807	10.0493	1.9826	N/A	N/A
Spike	N/A	2.2186	0.6836	10.6099	0.1871
Drop	N/A	1.8581	0.2288	10.6099	0.0356

the equatiosn of the regimes are presented in in (2.27) in Chapter 2.

Both the spike threshold TS and drop threshold TD are set as median of the de-deseasonalized ONR10s. The parameters of each regime are estimated and presented in Table 5.7, and the transition probabilities are presented in Table 5.8. The log-likelihood function of this estimation is -4951.7.

The estimated parameters in Table 5.7 show that the main characteristics of the price is captured. The positive mean-reversion rate β indicates the mean-reversion property in the price dynamics is captured by this model. The mean implied by the model is calculated from the estimated parameters. The model implied mean is 22.2244 for the spike regime, and is 4.0283 for the drop regime. The mean of the base regime is 10.0493, between the mean of the drop and spike regimes. The volatility σ of the spike regime is higher than the drop regime which reflects that the drops are more moderate.

Compared to the estimated parameters of the BSD model applied to log prices, the volatility parameter σ of the drop regime in Table 5.7 is much lower. On the other hand, σ of the spike regime is higher in the original price than that of the log price. These differences are consistent with the observations from the CDF curves in Figure 5.2 and 5.4 that the the original prices have more extreme spikes and less significant drops than the log prices.

The diagonal transition probabilities, which are the probability of keeping in the current regime, are above 0.5 for all three regimes. This implies the prices tends to stay in

Table 5.8: Estimated probability transition matrix of the three-regime base-spike-drop (BSD) model for ONR10s

Regime	Base	Spike	Drop
Base	0.9274	0.0615	0.0112
Spike	0.2595	0.7287	0.0118
Drop	0.2237	0.0832	0.6931

the current regime no matter what regime they currently resides in. This is a recognition of consecutive spikes as well as consecutive drops in the price time series. Another observation from Table 5.8 is that the transition probabilities between the spike and drop regimes are not zero. This is because in original prices, the price drops are relatively moderate so these prices are not significantly lower than the base regime. As a result, it is possible for the price to jump from a drop regime to a spike regime, and vice versa, although the probabilities are low. As shown in Table 5.7, the unconditional probabilities of the spike regime is 0.1871, while the unconditional probability of the drop regimes is 0.0356. The much higher probability of being in the spike regime is consistent with the observation in the price plot of the original prices.

The moments and quantile based measures for goodness-of-fit are calculated and presented in the Table 5.9. The results show that all these measures are fit very well. As shown in Table 5.6 and 5.9, the deviations with the two-regime BS model and three-regime BSD model are close. The log-likelihood function of the BSD model is higher than that of the BS model, but the difference is relatively small. This observation implies that adding the drop regime doesn't cause a significant improvement to goodness-of-fit for the studied original hourly reserve price. Given the benefits of a simpler model, for example, lower computation burden, the two-regime BS model is still a competitive candidate for the hourly reserve price studied.

Table 5.9: Statistical measures of goodness-of-fit with the three-regime base-spike-drop (BSD) model for ONR10s

	Mean	STD	IQR	IDR
Act	11.98	6.43	5.24	13.40
Sim	12.10	6.79	5.43	13.13
Dev	0.9%	5.58%	3.7%	-2.1%

5.4.4 Proposed three-regime base-spike-extreme model

As discussed in Section 5.4.1, the original reserve price has a relatively small number of drops, and the drops are moderate. The comparison in Section 5.4.3 shows that, although the BSD model has an extra drop regime compared to the BS model, it doesn't significantly improve in the goodness-of-fit. As a result, the drop regime may be unnecessary for the original hourly reserve price. On the other hand, a large number of positive spikes have been found in Figure 5.1, while some of them are relatively moderate and some of them are extremely high. Therefore, the positive spikes can be further divided into two groups. One group is the most extreme jumps which are even significantly higher than the other spikes. The other group of spikes are relatively lower and features relatively moderate fluctuations.

This observation inspires the idea of using two separate spike regimes to model these two distinguishing groups of spikes. The proposed three-regime base-spike-extreme (BSE) model has a base regime to model the normal state, a spike regime to model mild high prices and spikes, and an extreme regime to model the most extreme jumps. The base regime is modelled by an mean-reverting process. The spike and extreme regimes are modelled by two independent shifted Log-Normal distributions. TS and TE are thresholds for the spike and extreme regimes respectively. Only prices above TS can be captured by the spike regime, while the extreme regime only models prices above TE. TS is set to median to allow moderate high prices or spikes to be covered by the spike regime, and TE is set to 90% percentile so that only extremely high prices or spikes can be captured by the extreme regime. The equations of the three regimes are presented as follows: BSE model:

$$\text{Base Regime: } d(s(t)) = \beta(\mu - s(t-1))dt + \sigma dW_t \tag{5.1a}$$

$$\text{Spike Regime: } log(s(t) - TS) \sim N(\mu_s, \sigma_s) \tag{5.1b}$$

$$\text{Extreme Regime: } log(s(t) - TE) \sim N(\mu_e, \sigma_e) \tag{5.1c}$$

The three-regime BSE model is calibrated and the estimated parameters are shown in the tables below. The parameters are shown in Table 5.11. The log-likelihood function is -4721.8, which is the highest among the three models applied to hourly reserve price, indicating the best fit among the three models. The goodness-of-fit will be further compared and discussed later in this section.

Calculated from the estimated parameters, the mean of the spike regime implied by the model is 15.1495, and the mean of the extreme regime implied by the model is 28.3393. Also the volatility parameter σ is much higher in the extreme regime than in spike regime. These parameters show that the BSE model has successfully distinguished the extreme spikes and relatively moderate ones.

Compared to the parameters of the BSD model in Table 5.7, the base regime of the BSE model has a lower μ, the parameter of long term mean. This is because the base regime in the BSE model covers the low prices that were identified as drops in the BSD model.

Table 5.10: Estimated parameters of the three-regime base-spike-extreme (BSE) model for ONR10s

Regime	β	μ	σ	TS/TE	$Prob_s$ / $Prob_e$
Base	0.2722	9.4801	1.9631	N/A	N/A
Spike	N/A	1.3995	0.4761	10.6099	0.1635
Extreme	N/A	1.7642	0.8681	19.8314	0.0884

Transition probability matrix is in Table 5.11. The probability of staying in the current regime are again higher than inter-regime transition probabilities, indicating possibility of consecutive spikes. It worth noting that when the price is in the extreme regime, it has a higher probability to jump to spike regime rather than directly going back to the base regime. This is because an extreme spike usually occurs when the system is under contingent situation such as outages of major generation resources or transmission lines. The system operator would first apply short term solutions such as remedial action scheme shortly after the incident to relieve supply shortage or congestion. With these short term solutions, the price will reduce but may not fall back to the normal level until a permanent solution is in place (e.g. outage facilities back in service).

Table 5.11: Estimated probability transition matrix of the three-regime base-spike-extreme (BSE) model for log ONR10s

Regime	Base	Spike	Extreme
Base	0.9150	0.0670	0.0179
Spike	0.3123	0.5308	0.1569
Extreme	0.1412	0.3006	0.5581

The moments and percentile based measures are presented in Table 5.12 to evaluate goodness-of-fit. The four statistical measures are very well matched as all deviations are small. The results show that the moment-based measures are captured slightly better by the BSE model compared to the BS and BSD models, while IQR and IDR are matched slightly worse. In addition, this log-likelihood function of the BSE model is also higher than those of the BS and BSD models, which suggests the BSE model has an overall better fit than the other two models.

The identifications of the extreme and spike regimes are shown in a sample window of 2 weeks in Figure 5.5. It can be observed from this figure the probability of residing in the extreme regime, Prob(E), only increases to 1 when the price is above 20 \$/MWh, indicating that only extreme prices that are higher than TE can trigger the extreme regime. On the other hand, the extreme regime has also captured every peak prices in the plot. The spike

Table 5.12: Statistical measures of goodness-of-fit with the three-regime base-spike-extreme model for ONR10s

	Mean	STD	IQR	IDR
Act	11.98	6.43	5.24	13.40
Sim	12.03	6.58	5.55	12.66
Dev	0.4%	2.4%	6.0%	5.5%

regime tend to capture the relatively moderate high prices and the shoulders of the extreme prices, while the base regime only covers the low prices. This regime identification plot confirms that the three-regime BSE model successfully captures the moderate high prices and extreme prices by the spike and extreme regimes respectively.

5.4.5 Comparison with log price models

As discussed above, the three models applied to the original hourly reserve price have generally provided very good fit. In this section, the performance of these original price models are compared to the BSD model applied to log price. Since the log-likelihood functions can not be directly compared between two different data sets, only the four statistical measures, i.e., mean, standard deviation, IQR, and IDR, are compared.

The BSD model has outperformed the BS model when applied to log prices, and provide good match to the statistical measures except IQR. However, in the case of original price modelling, the goodness-of-fit with the BSD model and the BS model are comparable. In addition, the models applied to the original price have provided better matches to all statistical measure than the log price models, with the highest deviation of the studied measures being less than 6% for all the three original price models. The BSE model has provided the best overall fit among the three original price models.

The above comparison illustrates that the logarithmic transformation widely used in energy price modelling doesn't necessarily benefit the modelling of hourly reserve and reg-

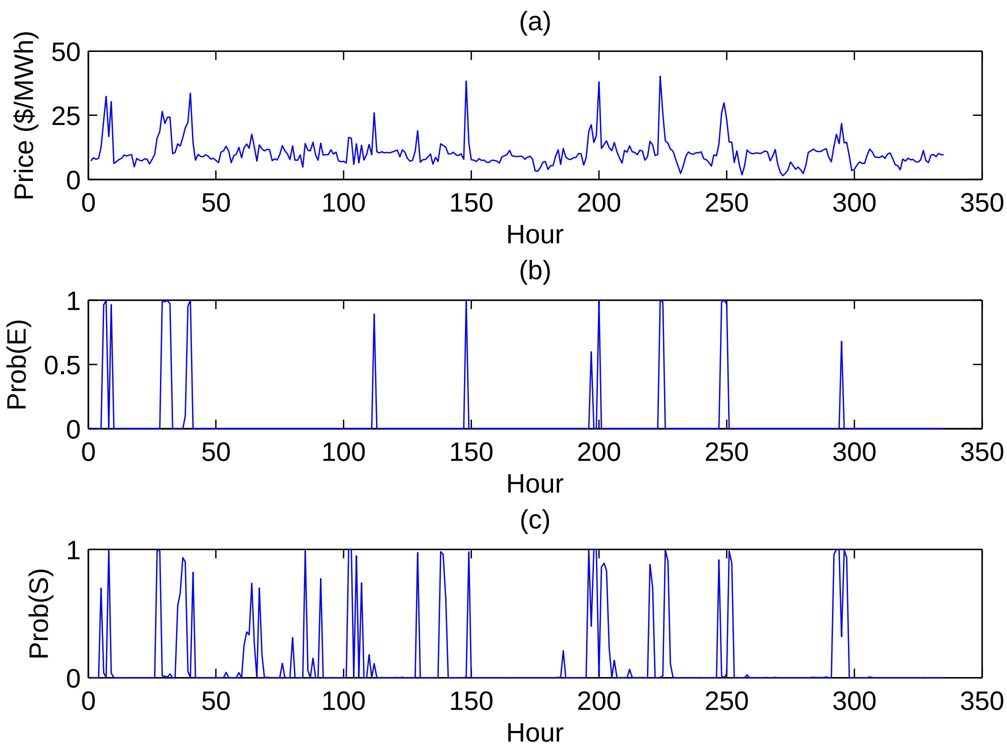

Figure 5.5: (a) Original de-seasonalized ONR10s (b) Probability of being in extreme regime with three-regime base-spike-extreme (BSE) model (c) Probability of being in spike regime with three-regime BSE model

ulation prices. These prices are generally much lower than energy price and may generate extreme negative spikes when taking logarithmic transformation. The original price can yield comparable or even better modelling accuracy than the log price.

5.5 Conclusion

In this chapter, modelling technique for hourly reserve price is investigated. Based on the characteristics of the hourly reserve price, models are built for both the log prices and original prices. For the log hourly reserve prices, a MRS three-regime base-spike-drop (BSD) model is applied and compared with a MRS two-regime base-spike model. The three-regime BSD model showed an obvious better fit to the log prices. However, due to the large amount of low prices in the studied reserve price process, the extreme negative drops generated in the logarithmic transformation has caused more challenges in price modelling.

The original price, on the other hand, has less extreme negative spikes but has more extreme positive spikes. Three MRS models have been applied to the studied original hourly reserve price. The two-regime base-spike model (BS) and three-regime base-spike-drop (BSD) that have been applied to the log price are tested for the original price. A new three-regime base-spike-extreme (BSE) model has been proposed in this chapter, which models the spikes by two regimes, distinguishing the most extreme spikes and the relatively mild spikes. Numerical simulation results show that the proposed BSE model outperforms the other two models and therefore is the more appropriate model.

The modelling of the log prices and the original prices have also been compared. The models applied to the original prices generally showed a better match to the statistical measures used to evaluate the goodness-of-fit, when compared to the log price models. Therefore, the simulation results from this chapter suggest that it is not necessary to take logarithmic transformation when modelling the hourly reserve price.

Chapter 6

Conclusions

Markets for operating reserves and regulation services are growing rapidly with the world-wide evolution of the electricity market as well as the development of renewable energy resources and the smart grid. This thesis explores the statistical characteristics and modelling of the reserve and regulation prices in three typical North American markets. The contributions of this work are to reveal the distinguishing characteristics of the reserve and regulation prices compared to energy prices, and find the appropriate stochastic models for these ancillary services prices. The findings in this thesis can provide useful information for market participants in their day to day operation and planning, such as bidding strategies and financial risk management.

In Chapter 3, the statistical characteristics of the reserve and regulation prices are quantified and compared with those of energy prices. The specific work that has been done in this chapter are:

1. Distributional features and patterns are analyzed for the studied reserve, regulation, and energy prices. These analyses provide an overview of the distribution and fluctuations of the studied prices.

2. The statistical characteristics including variability, jump frequency, extreme spikes, long-range correlation, and non-linearity are investigated, presenting significant differences between the energy prices and the reserve and regulation prices.

3. Relative variation index, which is a revised version of the historical volatility index, is proposed to evaluate the variability of reserve and regulation prices

to account for the zeros in these prices.

4. The origins of differences in characteristics are discussed considering the diversity in resource, demand, market mechanism and policy.

The main contributions and findings of Chapter 3 are as follows:

1. In the three studied markets, the reserve and regulation prices generally present lower price levels, larger dispersion, and different patterns compared to energy prices.

2. The variability of the reserve and regulation prices are generally significantly higher than these of energy prices. The high variability in reserve and regulation prices can be mainly attributed to the lower price level, lower demand level and thus the higher sensitivity to changes in supply, and discrete variation of the demand.

3. The reserve and regulation prices feature more frequent jumps and more extreme spikes. Moreover, the occurrence time of spikes in the reserve and regulation prices are not necessarily consistent with the energy prices due to different spike trigger schemes, which are then attributed to the differences in the definitions of supply and demand.

4. The reserve and regulation prices are both self-correlated, which indicates they are predictable. On the other hand, the correlations are smaller in these prices when compared to those of energy prices, which imply a weaker predictability. In addition, the non-linearity of reserve and regulation prices have been found higher than the energy prices.

The findings in this chapter provide an insight into the studied reserve and regulation prices, which is helpful to market participants in their bidding and planning to maximize profits. The characteristics of these prices are considered in Chapter 4 and Chapter 5 when modelling prices in the reserve and regulation market.

In Chapter 4, the dynamics of daily reserve and regulation prices are modelled, with the following work conducted:

1. Three stochastic models, MRJD model with independent jump component, MRS two-regime base-spike model, and MRS three-regime base-spike-drop model, are applied for daily reserve and regulation prices based on their characteristics.

2. The studied reserve and regulation prices are decomposed into deterministic and stochastic components, and the three selected models are applied to these prices.

3. The performance of models is compared using a selected set of indices. Comparisons have been made between models and between energy prices and reserve and regulation prices.

The main contributions and findings of Chapter 4 are as follows:

1. The three selected models have captured the main characteristics of the dynamics in reserve and regulation prices, such as mean-reversion and existence of jumps and spikes.

2. MRS models generally outperform the MRJD model because the MRS models provide a more flexible way of representing state transitions. The transitions of states have been reported to be a featuring characteristics of energy prices, but are more extreme in reserve and regulation prices. Therefore, the MRS models further outperform the MRJD models when applied to reserve and regulation prices.

3. The three-regime MRS base-spike-drop model adds a drop regime to capture drops and thus improves modelling accuracy. The reserve and regulation prices have lower price levels than the energy prices, and thus the drops are more significant in these prices after taking logarithmic transformation. The base-spike-drop model is an appropriate model for modelling log daily reserve and regulation prices.

In Chapter 5, price modelling has been extended to hourly prices of operating reserves and regulation services. The 10-minute spinning reserve in the Ontario market has been selected to be a typical reserve price and models are built and examined for this price. The main work of this chapter is:

1. The hourly reserve price is decomposed to a deterministic component and a stochastic component. MRS models are applied to the stochastic component.

2. In addition to the tradition of modelling log prices, the stochastic models are also applied to the original prices without logarithmic transformation.

3. A few selected MRS models with various specifications are applied to the hourly reserve price, and their performance is compared.

4. A new three-regime model has been proposed for modelling the original prices based on their distributional characteristics.

The main contributions and findings of Chapter 5 are as follows:

1. Compared to modelling of the daily prices, there are new challenges in modelling hourly prices due to their unique characteristics, such as larger dispersion, i.e., a larger span of price distribution compared to daily prices.

2. Although modelling log prices yields a reasonable fit, modelling original prices can be superior because the logarithmic transformation has made the distribution of the price significantly left-skewed.

3. The proposed three-regime model with two spike regimes have better captured the overall distribution of the studied original hourly reserve price. The proposed model outperforms the popular existing models, such as the MRS two-regime base-spike model and the MRS three-regime base-spike-drop model.

In Chapter 4, the three-regime base-spike-drop model is found to provide accurate descriptions of the daily reserve and regulation prices. In Chapter 5, the three-regime base-spike-extreme model applied to the original price has been found appropriate for the studied hourly prices.

The contribution and findings in this thesis are useful for electricity markets participants to understand the price characteristics, dynamics, and the impact of market condition changes on the reserve and regulation prices. The models built for daily and hourly prices can be further used by market participants to predict future price behaviour and evaluate their revenue streams manage risks involved in providing reserves and regulation service.

Bibliography

[1] K. Bhattacharya, M. H. Bollen, and J. E. Daalder, *Operation of Restructured Power Systems*. Norwell, MA: Kluwer Academic Publishers, 2001.

[2] D. S. Kirschen and G. Strbac, *Fundamentals of Power System Economics*. UK: Wiley, 2004.

[3] IESO, "Technical documents on the IESO electricity market." [Online]. Available: http://www.ieso.ca

[4] H. Zareipour, C. A. Canizares, and K. Bhattacharya, "The operation of Ontario's competitive electricity market: Overview, experiences, and lessons," *IEEE Transactions on Power Systems*, vol. 22, no. 4, pp. 1782–1793, NOV 2007.

[5] S. Stoft, "The demand for operating reserves: Key to price spikes and investment," *IEEE Transactions on Power Systems*, vol. 18, no. 2, pp. 470–477, MAY 2003.

[6] General Electric International Inc., "Ontario wind integration study - a report prepared for Ontario Power Authority (OPA), independent electricity system operator (IESO) and the canadian wind energy association (CanWEA)," Schenectady, NewYork, Tech. Rep., Oct 2006. [Online]. Available: http://www.ieso.ca/imoweb/pubs/marketreports/OPA-Report-200610-1.pdf

[7] H. Holttinen, P. Meibom, A. Orths, F. van Hulle, B. Lange, M. O'Malley, J. Pierik, B. Ummels, J. O. Tande, A. Estanqueiro, M. Matos, J. Ricardo, E. Gomez, L. Söder, G. Strbac, A. Shakoor, J. Richardo, J. C. Smith, M. Milligan, and E. Ela, "Design and operation of power systems with large amounts of wind power, Final report," IEA WIND Task 25, Tech. Rep., Phase one 2006-2008. [Online]. Available: http://www.vtt.fi/inf/pdf/tiedotteet/2009/T2493.pdf

[8] R. Sioshansi and P. Denholm. (2009) The value of plug-in hybrid electric vehicles as grid resources. [Online]. Available: http://iwse.osu.edu/isefaculty/sioshansi/papers/PHEV_V2G.pdf

[9] W. Kempton and J. Tomic, “Vehicle-to-grid power implementation: From stabilizing the grid to supporting large-scale renewable energy,” *Journal of Power Sources*, vol. 144, no. 1, pp. 280–294, Jun. 2005.

[10] J. Arroyo and A. Conejo, “Optimal response of a power generator to energy, AGC, and reserve pool-based markets,” *IEEE Transactions on Power Systems*, vol. 17, no. 2, pp. 404–410, MAY 2002.

[11] H. Haghighat, H. Seifi, and A. R. Kian, “On the self-scheduling of a power producer in uncertain trading environments,” *Electric Power Systems Research*, vol. 78, no. 3, pp. 311–317, MAR 2008.

[12] T. Li, M. Shahidehpour, and Z. Li, “Risk-constrained bidding strategy with stochastic unit commitment,” *IEEE Transactions on Power Systems*, vol. 22, no. 1, pp. 449–458, FEB 2007.

[13] V. Vahidinasab and S. Jadid, “Stochastic multiobjective self-scheduling of a power producer in joint energy and reserves markets,” *Electric Power Systems Research*, vol. 80, no. 7, pp. 760–769, JUL 2010.

[14] D. J. Swider and C. Weber, “Bidding under price uncertainty in multi-unit pay-as-bid procurement auctions for power systems reserve,” *European Journal of Operational Research*, vol. 181, no. 3, pp. 1297–1308, SEP 16 2007.

[15] W. Kempton and J. Tomic, “Vehicle-to-grid power fundamentals: calculating capacity and net revenue,” *Journal of Power Sources*, vol. 144, no. 1, pp. 268–279, Sep. 2005.

[16] J. Short and P. Denholm, "A preliminary assessment of plug-in hybrid electric vehicles on wind energy markets," National Renewable Energy Labratory (NREL), U.S. Department of Energy, washington, DC, Tech. Rep., Apr. 2006.

[17] S. Han, S. Han, and K. Sezaki, "Development of an: Optimal vehicle-to-grid aggregator for frequency regulation," *IEEE Transactions on Smart Grid*, vol. 1, no. 1, pp. 65 – 72, June. 2010.

[18] M. H. Albadi and E. F. El-Saadany, "Overview of wind power intermittency impacts on power systems," *Electric Power Systems Research*, vol. 80, no. 6, pp. 627–632, JUN 2010.

[19] R. Doherty and M. O'Malley, "A new approach to quantify reserve demand in systems with significant installed wind capacity," *IEEE Transactions on Power Systems*, vol. 20, no. 2, pp. 587–595, MAY 2005.

[20] GWEC, "Global wind 2008 report," Global Wind Energy Council, Technical Report, 2009.

[21] D. J. Swider and C. Weber, "The costs of wind's intermittency in germany: application of a stochastic electricity market model," *European Transactions on Electrical Power*, vol. 17, no. 2, pp. 151–172., 2007.

[22] J. MacCormack, A. Hollis, H. Zareipour, and W. Rosehart, "The large-scale integration of wind generation: Impacts on price, reliability and dispatchable conventional suppliers," *Energy Policy*, vol. 38, no. 7, pp. 3837 – 3846, 2010.

[23] I. Simonsen, "Volatility of power markets," *Physica A: Statistical Mechanics and its Applications*, vol. 355, no. 1, pp. 10–20, SEP 1 2005.

[24] Y. Li and P. Flynn, "Deregulated power prices: comparison of volatility," *Energy Policy*, vol. 32, no. 14, pp. 1591–1601, SEP 2004.

[25] H. Zareipour, K. Bhattacharya, and C. A. Canizares, "Electricity market price volatility: The case of Ontario," *Energy Policy*, vol. 35, no. 9, pp. 4739–4748, SEP 2007.

[26] R. Weron, M. Bierbrauer, and S. Truck, "Modeling electricity prices: jump diffusion and regime switching," *Physica A: Statistical Mechanics and its Applications*, vol. 336, no. 1-2, pp. 39–48, MAY 1 2004.

[27] I. Simonsen, R. Weron, and B. Mo, "Structure and stylized facts of a deregulated power market," 2004. [Online]. Available: http://mpra.ub.uni-muenchen.de/1443

[28] R. Weron, *Modeling and Forecasting Electricity Loads and Prices: A Statistical Approach*. The Atrium, Southern Gate, Chichester, West Sussex PO19 8SQ, England: John Wiley & Sons Ltd, 2006.

[29] J. Alvarez-Ramirez, R. Escarela-Perez, G. Espinosa-Perez, and R. Urrea, "Dynamics of electricity market correlations," *Physica A: Statistical Mechanics and its Applications*, vol. 388, no. 11, pp. 2173–2188, JUN 1 2009.

[30] D. J. Swider and C. Weber, "Extended ARMA models for estimating price developments on day-ahead electricity markets," *Electric Power Systems Research*, vol. 77, no. 5-6, pp. 583–593, APR 2007.

[31] D. Moest and D. Keles, "A survey of stochastic modelling approaches for liberalised electricity markets," *European Journal of Operational Research*, vol. 207, no. 2, pp. 543–556, DEC 1 2010.

[32] J. Lucia and E. Schwartz, "Electricity prices and power derivatives: Evidence from the nordic power exchange," *Review of Derivatives Research*, vol. 5, pp. 5 – 50, 2002.

[33] S. Borovkova and F. Permana, "Modelling electricity prices by the potential jump-diffusion," in *Stochastic Finance*. 233 Spring Street, New York, NY 10013, United States: Springer, 2006, Proceedings Paper, pp. 239–263.

[34] R. Huisman and R. Mahieu, "Regime jumps in electricity prices," *Energy Economics*, vol. 25, no. 5, pp. 425–434, SEP 2003.

[35] C. Knittel and M. Roberts, "An empirical examination of restructured electricity prices," *Energy Economics*, vol. 27, no. 5, pp. 791–817, SEP 2005.

[36] R. Weron, "Market price of risk implied by Asian-style electricity options and futures," *Energy Economics*, vol. 30, no. 3, pp. 1098–1115, MAY 2008.

[37] H. Higgs and A. Worthington, "Stochastic price modeling of high volatility, mean-reverting, spike-prone commodities: The Australian wholesale spot electricity market," *Energy Economics*, vol. 30, no. 6, pp. 3172–3185, NOV 2008.

[38] C. De Jong, "The nature of power spikes: A regime-switch approach," *Studies in Nonlinear Dynamics and Econometrics*, vol. 10, no. 3, OCT 2006.

[39] R. Weron, "Heavy-tails and regime-switching in electricity prices," *Mathematical Methods of Operations Research*, vol. 69, no. 3, pp. 457–473, JUL 2009.

[40] C. Mari, "Regime-switching characterization of electricity prices dynamics," *Physica A - Statistical Mechanics And Its Applications*, vol. 371, no. 2, pp. 552–564, NOV 15 2006.

[41] J. Janczura and R. Weron, "An empirical comparison of alternate regime-switching models for electricity spot prices," *Energy Economics*, vol. 32, no. 5, pp. 1059–1073, SEP 2010.

[42] S. Schlueter, “A long-term/short-term model for daily electricity prices with dynamic volatility,” *Energy Economics*, vol. 32, no. 5, pp. 1074–1081, SEP 2010.

[43] F. Olsina and C. Weber, “Stochastic Simulation of Spot Power Prices by Spectral Representation,” *IEEE Transactions on Power Systems*, vol. 24, no. 4, pp. 1710–1719, NOV 2009.

[44] l. Cartea and M. G. Figueroa, “Pricing in electricity markets: A mean reverting jump diffusion model with seasonality,” *Applied Mathematical Finance*, vol. 12, no. 4, pp. 313–335, 2005.

[45] T. Christensen, S. Hurn, and K. Lindsay, “It Never Rains but it Pours: Modeling the Persistence of Spikes in Electricity Prices,” *Energy Journal*, vol. 30, no. 1, pp. 25–48, 2009.

[46] M. Bierbrauer, S. Truck, and R. Weron, “Modeling electricity prices with regime switching models,” in *Computational Science - ICCS 2004, Proceedings*, Bubak, M and DickVanAlbada, G and Sloot, PMA and Dongarra, JJ, Ed., vol. 3039, no. Part 4, 2004, pp. 859–867.

[47] J. Janczura and R. Weron, “Regime-switching models for electricity spot prices: Introducing heteroskedastic base regime dynamics and shifted spike distributions,” in *Energy Market, 2009. EEM 2009. 6th International Conference on the European*, may 2009, pp. 1 –6.

[48] H. Geman and A. Roncoroni, “Understanding the fine structure of electricity prices,” *The Journal of Business*, vol. 79, no. 3, pp. 1225–1261, MAY 2006. [Online]. Available: http://www.jstor.org/stable/10.1086/500675

[49] R. Weron and A. Misiorek, “Forecasting spot electricity prices: A comparison of parametric and semiparametric time series models,” *International Journal of Forecasting*,

vol. 24, no. 4, pp. 744 – 763, 2008.

[50] N. V. Karakatsani and D. W. Bunn, "Intra-day and regime-switching dynamics in electricity price formation," *Energy Economics*, vol. 30, no. 4, pp. 1776–1797, JUL 2008.

[51] R. Becker, S. Hurn, and V. Pavlov, "Modelling spikes in electricity prices," *The Economic Record*, vol. 83, no. 263, pp. 371–382, DEC 2007.

[52] F. Nogales, J. Contreras, A. Conejo, and R. Espinola, "Forecasting next-day electricity prices by time series models," *IEEE Transactions on Power Systems*, vol. 17, no. 2, pp. 342–348, MAY 2002.

[53] C. Garcia-Martos, J. Rodriguez, and M. Sanchez, "Mixed models for short-run forecasting of electricity prices: Application for the spanish market," *IEEE Transactions on Power Systems*, vol. 22, no. 2, pp. 544–552, May 2007.

[54] P. Wang, H. Zareipour, and W. D. Rosehart, "Characteristics of the prices of operating reserves and regulation services in competitive electricity markets," *Energy Policy*, vol. 39, no. 6, pp. 3210–3221, JUN 2011.

[55] J. C. Hull, *Options, Futures, and Other Derivatives*, 4th ed. Upper Saddle River, NJ 07458: Prentice Hall, 2000.

[56] P. F. Christoffersen, *Elements of Financial Risk Managemen*. 525 B Street, Suite 1900, San Diego, California 92101-4495, USA: Academic Press, 2003.

[57] C. Peng, S. Havlin, H. Stanley, and A. Goldberger, "Quantification of scaling exponents and crossover phenomena in nonstationary heartbeat time series," *Chaos*, vol. 5, no. 1, pp. 82–87, MAR 1995.

[58] J. Kantelhardt, S. Zschiegner, E. Koscielny-Bunde, S. Havlin, A. Bunde, and H. Stanley, “Multifractal detrended fluctuation analysis of nonstationary time series,” *Physica A: Statistical Mechanics and its Applications*, vol. 316, no. 1-4, pp. 87–114, DEC 15 2002.

[59] C. d. Jong and R. Huisman, “Option formulas for mean-reverting power prices with spikes,” Erasmus Research Institute of Management (ERIM), Research Paper ERS-2002-96-F&A, Oct. 2002. [Online]. Available: http://ideas.repec.org/p/dgr/eureri/2002251.html

[60] J. Hamilton, “Regime-switching models,” *Prepared for: Palgrave Dictionary of Economics*, 2005.

[61] C.-J. Kim, “Dynamic linear models with markov-switching,” *Journal of Econometrics*, vol. 60, no. 12, pp. 1 – 22, 1994.

[62] R. Weron and J. Janczura, “Efficient estimation of markov regime-switching models: An application to electricity wholesale market prices,” University Library of Munich, Germany, MPRA Paper 26628, Nov. 2010. [Online]. Available: http://ideas.repec.org/p/pra/mprapa/26628.html

[63] R. Billinton and R. N. Allan, *Reliability Evaluation of Engineering Systems: Concepts and Techniques*, 2nd ed. 233 Spring Street, New York, N.Y. 10013: Springer, 1992, 1992.

[64] NYISO, “Technical documents of the New York electricity market.” [Online]. Available: http://www.nyiso.com/

[65] NYISO, “NYISO Ancillary Service Manual.” [Online]. Available: http://www.nyiso.com/public/webdocs/documents/manuals/operations/ancserv.pdf

[66] ERCOT, "Technical documents of the ERCOT electricity market." [Online]. Available: http://www.ercot.com

[67] A. G. Isemonger, "The evolving design of RTO ancillary service markets," *Energy Policy*, vol. 37, no. 1, pp. 150–157, JAN 2009.

[68] Ontario Energy Board, "Ontario Market Surveillance Panel Monitoring Reports." [Online]. Available: http://www.ontarioenergyboard.ca/OEB/Industry/About+the+OEB/Electricity+Market+Surveillance/Market+Surveillance+Panel+Reports

[69] NYISO, "2008 State of Market Report - New York ISO." [Online]. Available: http://www.nyiso.com/public/webdocs/documents/market$_$advisor$_$reports/2008/NYISO$_$2008$_$SOM$_$Final$_$9-2-09.pdf

[70] CAISO, "CAISO Market issues and performance reports." [Online]. Available: http://www.caiso.com/market/Pages/MarketMonitoring/MarketIssuesPerfomanceReports/Default.aspx

[71] G. E. P. Box and G. M. Jenkins, *Time Series Analysis: Forecasting and Control*. 500 Sansome Street, San Francisco, California: Holden-Day Inc., 1976.

[72] S. Riedel and H. Weigt, "German Electricity Reserve Markets," 2007, Electricity Markets Working Paper No. WP-EM-20, Technical University of Dresden. [Online]. Available: http://www.hannesweigt.de/paper/wp$_$em$_$20$_$riedel$_$weigt$_$Germany$_$reserve$_$markets.pdf

[73] J. H. Zhao, Z. Y. Dong, X. Li, and K. P. Wong, "A framework for electricity price spike analysis with advanced data mining methods," *IEEE Transactions on Power Systems*, vol. 22, no. 1, pp. 376–385, FEB 2007.

[74] J. H. Zhao, Z. Y. Dong, and X. Li, “Electricity market price spike forecasting and decision making,” *IET Generation, Transmission and Distribution*, vol. 1, no. 4, pp. 647–654, JUL 2007.

[75] M. Bierbrauer, C. Menn, S. T. Rachev, and S. Truck, “Spot and derivative pricing in the EEX power market,” *Journal of Banking & Finance*, vol. 31, no. 11, pp. 3462–3485, NOV 2007.